Kojima et al. (28), rOAT2 was identified as the ~60-kDa protein equally distributed in the cortical, outer medullary and inner medullary tissue and immunolocalized to the apical membrane of thick ascending limb of Henle (TALH) and cortical and medullary collecting ducts (CD) in the rat kidney, whereas hOAT2 was immunolocalized to the proximal tubule basolateral membrane in the human kidney (13). In the mouse kidney, mOAT2 was recently localized to the luminal membrane of proximal tubules in the M animal (25). In this work, we reinvestigated expression of the rOAT2-specific mRNA in the kidneys of M, F, and variously treated M rats by RT-PCR and performed a detailed immunolocalization of this transporter along the rat and mouse nephron by using an affinity-purified, polyclonal anti-peptide antibody that reacted with OAT2 in both species.

MATERIAL AND METHODS

Animals and treatment. Prepubertal (age: 20–25 days), young (age: 6 wk), and adult (age: 11–12 wk) M and F Wistar strain rats were from the breeding colony at the Institute in Zagreb. Animals were bred and maintained according to the Guide for Care and Use of Laboratory Animals (National Research Council). Before and during experiments, animals had free access to standard pelleted food and tap water. The studies were approved by the Ethics Committee of the Institute of Medical Research and Occupational Health.

Prepubertal rats were used intact, and young M rats were sham operated or gonadectomized, whereas adult rats were used either intact, sham operated, or gonadectomized. M rats were castrated by a scrotal route, whereas F rats were ovariectomized by the dorsal (lumbal) approach under proper anesthesia [Narketan (80 mg/kg body mass)-Xylapan (12 mg/kg body mass), ip]. The sham-operated animals underwent the same procedure, except the respective organs were not removed.

The castrated, ovariectomized, and sham-operated adult rats were left to recover for 4 wk before death. The young M rats were castrated or sham operated; 6 wk later, the castrated animals underwent a subcutaneous treatment with either testosterone enanthate or estradiol dipropionate, or progesterone at a dose of (each) 2.5 mg·kg body mass^{-1}·day^{-1} for 14 days. The hormones were injected as a sunflower oil solution. The castrated control and sham-operated rats were treated with an equivalent amount of sunflower oil (0.5 ml·kg body mass^{-1}·day^{-1} for 14 days).

Antibodies and other material. An immune serum against the peptide sequence in the COOH-terminal domain of the protein (amino acids 512–528: ETKKAQLPETIQDVERK), which is common to rOAT2 (GenBank: NP_445989.1 for *Rattus norvegicus*) and mOAT2 (GenBank: NP_659105.1 for *Mus musculus*), was raised in rabbits, and the antibody (rOAT2-Ab) was purified using an affinity column. Compared with the previously described antibody (28), the rOAT2-Ab used in the present study was *1*) raised against the same peptide sequence but in different rabbits showing higher antibody titer following immunization (ELISA data not shown) and *2*) tested by an optimized processing of isolated membranes in Western blotting experiments and antigen retrieval technique in tissue cryosection (see below). The antibody was kindly supplied by Transgenic, Kumamoto, Japan. The use of affinity-purified polyclonal antibodies for Na-K-ATPase and water channel aquaporin-1 (AQP1) was described in our previous publications (42, 44). A monoclonal antibody against α-actin was purchased commercially (Chemicon International, Temecula, CA). Secondary antibodies, including the CY3-labeled (GARCY3) and alkaline phosphatase-labeled goat anti-rabbit (GARAP) or anti-mouse IgG (GAMAP) antibodies, were purchased from Jackson ImmunoResearch Laboratories, (West Grove, PA) or Kirkegaard and Perry (Gaithersburg, MD).

Anesthetics (Narketan and Xylapan) were purchased from Chassot, Bern, Switzerland. Oil solutions of testosterone enanthate, estradiol dipropionate, and progesterone were from RotexMedica (Trittau, Germany) and Galenika (Belgrade, SCG). The reagents and kits for RNA isolation and RT-PCR were obtained commercially; RNALater was from Sigma-Aldrich (Taufkirchen, Germany), Trizol and DNase/RNase-free water were from Gibco-BRL (Grand Island, NY), First Strand cDNA Synthesis Kit was from Fermentas International (Burlington, ON, Canada), whereas custom primers for rOAT2 and β-actin were from Invitrogen (online). Various other chemicals were of the highest purity available and were purchased from either Sigma (St. Louis, MO) or Fisher Scientific (New Jersey, NJ).

Isolation of RNA and RT-PCR. The animals were killed by decapitation. The kidneys were removed, decapsulated, and cut into 1-mm-thick sagital slices. One slice was immediately submerged into the RNAlater solution for manual separation of the cortical and outer stripe tissues. Total cellular RNA from these zones was extracted using Trizol according to the manufacturer's instructions. RNA concentration and its purity were estimated by spectrophotometric measurement of the optical density at 260/280 nm. The quality and integrity of RNAs were tested by agarose gel electrophoresis. Isolated RNAs were stored at −70°C until use. To perform RT-PCR, first-strand cDNA synthesis was performed using the First Strand cDNA Synthesis Kit following the prescribed instructions. Total cellular RNA (3 μg) was denatured at 70°C for 5 min in reaction mixture containing 0.5 μg oligo(dT)$_{18}$ and reverse transcribed in a total volume of 20 μl of reaction mixture containing 1× reverse transcription buffer, 20 units of ribonuclease inhibitor, 1 mM dNTPmix, and 40 units of Moloney murine leukemia virus (M-MuLV) RT. The reaction mixture was then incubated at 37°C for 60 min, followed by incubation at 72°C for 10 min. cDNAs were diluted 5× in DNase/RNase-free water and stored at −20°C until use. PCR was performed in total volume of 20 μl using 1 μl of 5×-diluted first-strand cDNA, 0.4 μM rOAT2-specific primers, and ready-to-use PCR Master Mix, following instructions from the manufacturer. The housekeeping gene β-actin was used as a control for variations in the input of RNA. The sequences of specific forward and reverse rOAT2 and β-actin primers used for RT-PCR reactions, and predicted RT-PCR product sizes, are listed in Table 1. To avoid amplification of genomic DNA, the intron overspanning primers were used. The reaction conditions used for

Table 1. *Primer sequences used for RT-PCR*

Forward and Reverse Primers (5′-3′)	GenBank Accession No.	Location	RT-PCR Product Size, bp
	rOAT2		
F: CGCTCAGAATTCTCCTCCAC	NM_053537.1	434–453	311
R: ACATCCAGCCACTCCAACTC		725–744	
	β-Actin		
F: GTCGTACCACTGGCATTGTG	NM_031144.2	518–537	364
R: AGGAAGGAAGGCTGGAAGAG		862–881	

Genes: rat ortholog of organic anion transporter-2 (rOAT2) and β-actin. F, forward; R, reverse.

PCR were as follows: initial denaturation for 3 min at 94°C, denaturation for 30 s at 95°C, annealing for 30 s at 95°C, and elongation for 45 s at 72°C, with 32 and 30 cycles for OAT2 and β-actin, respectively. The nontemplate control (NTC) reactions, where the cDNA was substituted with DNase/RNase-free water, were included in each PCR reaction to screen for possible contamination; no PCR products were detected in NTC reaction, indicating the absence of possible contamination (data not shown). RT-PCR products were resolved by electrophoresis in 1% agarose gel, stained with ethidium bromide, and visualized under ultraviolet light. To obtain quantitative results, preliminary experiments were done to determine the optimal number of PCR cycles within the exponential phase of the PCR reaction (data not shown).

Tissue fixation and immunocytochemistry. The animals were anesthetized, and the circulatory system was perfused via the left ventricle of the heart using the Masterflex pump (Cole-Parmer, Chicago, IL), first with aerated (95% O_2-5% CO_2) and temperature-equilibrated (37°C) phosphate-buffered saline (PBS; in mM: 137 NaCl, 2.7 KCl, 8 Na_2HPO_4, 2 K_2PO_4, pH 7.4) for 2–3 min to remove blood, and then with 10 ml (mice) or 150 ml (rats) of fixative (4% paraformaldehyde in PBS) for 4–5 min. The kidneys were removed, sliced, and kept overnight in the same fixative at 4°C, followed by extensive washing in PBS and storage in PBS containing 0.02% NaN_3 at 4°C until further use.

To cut 4-μm frozen sections, tissue slices were infiltrated with 30% sucrose (in PBS) overnight, embedded in the Jung Tissue Freezing Medium (Leica Microsystems, Nussloch, Germany), frozen at −25°C, and sectioned in a Leica CM 1850 cryostat (Leica Instruments, Nussloch, Germany). Sections were collected on Superfrost/Plus Microscope slides (Fischer Scientific), dried at room temperature for 2–3 h, and kept refrigerated until further use.

An antigen retrieval technique was used to maximize the antibody-binding sites. In preliminary studies, we tried different methods to process tissue cryosections before immunostaining, including *1*) pretreatment without or with ionic (SDS) or nonionic detergents (Triton X-100) that were previously used to reveal cryptic Na-K-ATPase and vacuolar H^+-ATPase (5, 43), *2*) pretreatment with xylol and graded concentrations of ethanol (steps used for antigen retrieval in paraffin sections) without or with microwave heating in citrate buffers of different pH that were found to be optimal for revealing OAT1 and OAT3 in the rat kidney (32), and *3*) pretreatment with microwave heating only in citrate buffers of different pH, 3, 6, or 9, without or with 0.5% Triton X-100. The immunostaining efficiency following these procedures was very heterogeneous (data not shown). The following procedure gave the strongest immunostaining of OAT2 in the rat and mouse cryosections: sections were rehydrated in PBS for 15 min, heated in 10 mM citrate buffer, pH 6, in a microwave oven (4 cycles, 5 min each at 800 W), followed by cooling down to room temperature in the same buffer for 20 min. Further steps were performed in a wet chamber: sections were incubated with 0.5% Triton X-100 (in PBS) for 5 min, rinsed with PBS (5 × 5 min each), incubated for 20 min with bovine serum albumin (1% BSA in PBS) to block the nonspecific antibody binding, incubated with the rOAT2-Ab (diluted 1:2,000 with PBS) overnight in a refrigerator, rinsed with PBS (4 × 5 min each), incubated with GARCY3 (1.6 μg/ml in PBS) at room temperature for 60 min, rinsed with PBS (4 × 5 min each), and mounted in a fluorescence fading retardant (Vectashield; Vector Laboratories, Burlingame, CA).

To test the staining specificity, rOAT2-Ab was blocked with the immunizing peptide (final concentration of the peptide, 0.5 mg/ml) for 4 h at room temperature before use in the above-described immunofluorescence assay.

The stained sections were examined and photographed with an Opton III RS fluorescence microscope (Opton Feintechnik, Oberkochen, Germany) using a Spot RT Slider camera and software (Diagnostic Instruments, Sterling Heights, MI). The photos were imported into Adobe Photoshop 6.0 for processing and labeling.

Preparation of tissue homogenates and membranes. Animals were killed by decapitation. Mouse kidneys were used in toto. Rat kidneys were removed and sagitally sliced, and their cortex and outer stripe were dissected manually and used as separate tissue pools, while the inner stripe and inner medulla were processed as a single sample. The respective tissue was homogenized (10% homogenate) in a chilled buffer (in mM: 300 mannitol, 5 EGTA, 12 Tris·HCl, pH 7.4, 1 phenylmethylsulfonyl fluoride, and 0.1 benzamidine and 0.1 μg/ml antipain) with a Powergen 125 homogenizer (Fisher Scientific) at maximal setting (1-min homogenization, 1-min pause, 1-min homogenization). The total cell membranes (TCM) were isolated from the homogenate by first removing cell debris by centrifugation in a refrigerated high-speed centrifuge (Sorvall RC-5C; Sorvall Instruments, Newtown, CT; rotor SS34) at 6,000 *g* for 15 min. The pellet was discarded, and the supernatant was then centrifuged at 150,000 *g* for 1 h (ultracentrifuge Sorvall OTD-Combi, rotor T-875). The final pellet (TCM) was resuspended in homogenizing buffer.

The homogenates of cortical and outer stripe tissues of the rat kidney and the whole mouse kidney homogenates were used to isolate brush-border membranes (BBM) by Mg^{2+}-EGTA precipitation (1). After dispersion of membranes in an appropriate volume of buffer (150 mM mannitol, 6 mM EGTA, 6 mM HEPES-Tris, pH 7.4) and measurement of proteins by the Bradford assay (2), all membrane preparations were stored at −70°C until further use for immunoblotting studies.

SDS-PAGE and Western blotting. The membrane samples were thawed at 37°C and mixed with sample buffer, which in a final mixture contained the following: 1% SDS, 12% vol/vol glycerol, 30 mM Tris·HCl, pH 6.8, without (nonreducing conditions) or with 5% β-mercaptoethanol (β-ME; reducing conditions). Samples were denatured at 95°C for 5 min, 65°C for 15 min, or 37°C for 30 min. Proteins were separated through 10% SDS-PAGE minigels using the Vertical Gel Electrophoresis System and then electrophoretically wet-transferred using a Mini Trans-Blot Electrophoretic Transfer Cell (both Bio-Rad Laboratories, Hercules, CA) to an Immobilon membrane (Millipore, Bedford, MA). The amount of protein per lane was 30–40 μg for BBM and 60–80 μg for TCM; the exact amount of protein per lane is indicated in figure legends. Following transfer, the Immobilon membrane was briefly stained with Coomassie Brilliant Blue to check for the efficiency of transfer, destained, blocked in blotting buffer (5% nonfat dry milk, 0.15 M NaCl, 1% Triton X-100, 20 mM Tris·HCl, pH 7.4), and incubated at 4°C overnight (12–14 h) in the same buffer containing either rOAT2-Ab (1:2,000), anti-Na-K-ATPase antibody (1:1,000), or anti-AQP1 antibody (1:10,000). In some experiments, to check for proper loading and transfer, the lower part of the stained transfer membrane was cut off, destained, blocked in blotting buffer, and probed for α-actin by incubation at 4°C overnight in the anti-α-actin antibody (1:1,000 in blotting buffer). Then the membranes were washed with blotting buffer (4 × 15 min), incubated for 60 min in the same buffer that contained GARAP (0.1 μg/ml) or GAMAP (0.5 μg/ml), washed again, and stained for alkaline phosphatase activity using the color-developing assay that contained 5-bromo-4-chloro-3-indolyl phosphate (BCIP; 1.65 mg/ml) and nitro blue tetrazolium (NBT; 3.3 mg/ml) in 20 mM Tris·HCl buffer, pH 9.0.

The labeled rOAT2-related protein band, estimated at ~66 kDa by use of commercial protein markers (Gibco-BRL), was evaluated by densitometry. The intensity of the labeled band was scanned (Ultroscan Laser Densitometer; LKB, Bromma, Sweden), and the integrated surface of each scan was expressed in arbitrary units, relative to the strongest band density (=1,00 unit) in the corresponding control samples.

Presentation of the data. The RT-PCR data were obtained with RNA preparations from two animals of each experimental group, whereas the immunocytochemical and immunoblotting data represent findings in four to five animals in each experimental group. The numeric data, expressed as means ± SE, were statistically evaluated

by use of Student's *t*-test or ANOVA with Duncan's test at the 5% level of significance.

RESULTS

Expression of OAT2-specific mRNA in rat kidney. Previous studies with various methods, including Northern blotting, branched DNA analysis, and RT-PCR, described gender differences in the renal expression of rOAT2 (F > M) in sexually matured rats (6, 7, 24, 29). Following castration in M rats, the rOAT2 transcript in the kidney was either upregulated (24, 29) or unchanged (7), and the treatment of castrated M with testosterone or estrogen downregulated, whereas ovariectomy in F either had no effect (29) or slightly downregulated (7), the renal rOAT2 expression. Although partially contradictory, overall these data indicate that gender differences in the renal expression of rOAT2 mRNA in rats might be caused by androgen inhibition and estrogen stimulation. To reinvestigate these data, we have isolated RNA from the kidney outer stripe tissue (it exhibits the highest expression of rOAT2 protein; see below) of sham-operated and gonadectomized M and F rats, and of castrated M treated with oil (control) or various sex steroids, and compared the rOAT2-specific mRNA expression by RT-PCR (Fig. 1).

As shown in Fig. 1*A*, the sham-operated F exhibited a higher expression of rOAT2 mRNA than the sham-operated M, proving the presence of gender differences (F > M). Castration upregulated, whereas ovariectomy downregulated, the rOAT2 mRNA expression, indicating that androgens acted inhibitory and estrogens stimulatory. These findings were further confirmed by treating castrated M with testosterone, which resulted in downregulation, and with estradiol or progesterone, which caused an upregulation of rOAT2 (Fig. 1*B*). The expression of β-actin mRNA was unchanged in all experimental conditions. Similar, but more heterogeneous, data were observed for mRNA expression in the renal cortical tissue from the same animals (data not shown).

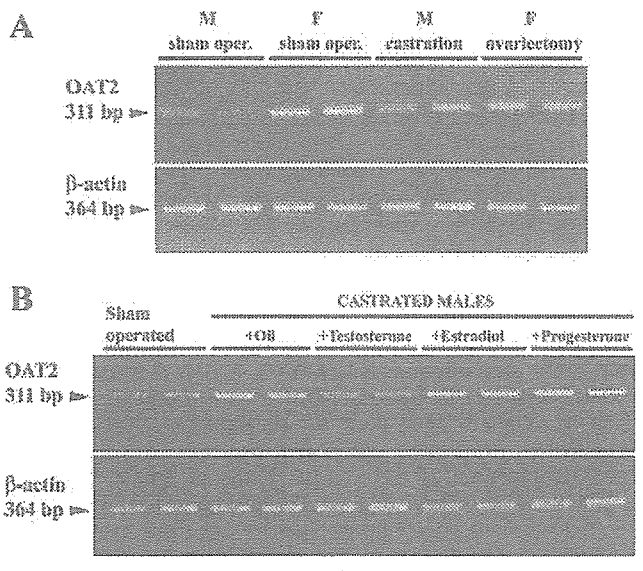

Fig. 1. RT-PCR data showing the expression of rat organic anion transporter-2 (rOAT2)- and β-actin-specific mRNAs. *A*: the kidney outer stripe tissue of sham-operated and gonadectomized male (M) and female (F) rats. *B*: the castrated M treated with oil (control) or various sex hormones. Each band represents mRNA expression in the tissue from a separate animal. The data prove gender differences in the renal OAT2 mRNA expression (F > M), its upregulation by castration and downregulation by ovariectomy (*A*), and its downregulation by testosterone and upregulation by estradiol and progesterone treatment (*B*). The expression of β-actin mRNA was similar in renal tissues from both sexes and remained unaffected by the hormonal treatment.

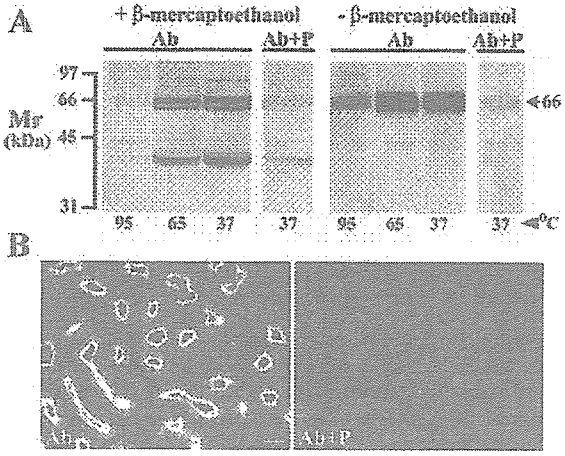

Fig. 2. Testing of rOAT2-Ab specificity by immunoblotting (*A*) and immunocytochemistry (*B*) in the samples from rat kidney. *A*: total cell membranes, isolated from the F kidney outer stripe homogenate, were prepared in reducing (+β-mercaptoethanol) or nonreducing (−β-mercaptoethanol) conditions at the indicated heating temperatures for 5 min (95°C), 15 min (65°C), or 30 min (37°C) and blotted with the rOAT2-Ab (Ab) or with the antibody that had been preincubated with the immunizing peptide (Ab+P). Two major protein bands (~40 and ~66 kDa) were labeled in reducing conditions, whereas only one band (~66 kDa) was labeled in nonreducing conditions. In both conditions, the bands increased with decreasing temperature and were largely blocked by the peptide. Each lane contained 60 μg of protein. *B*: by immunocytochemistry, brush border of the proximal tubule S3 segment in the outer stripe was strongly stained (Ab), and this staining was blocked by the immunizing peptide (Ab+P).

Specificity of rOAT2-Ab in immunoblotting and immunocytochemical studies with the samples from rat kidney. Before detailed immunolocalization of the rOAT2 protein in rat kidney was performed, the rOAT2-Ab specificity was tested by immunoblotting TCM preparations from the F kidney outer stripe homogenate and by immunostaining cryosections of the same tissue. Different experimental conditions were applied, without or with inactivation of the rOAT2-Ab with the immunizing peptide. As shown in Fig. 2*A*, in reducing conditions, the antibody consistently labeled two protein bands, at ~40 kDa and ~66 kDa, that were strongest after heating at 37°C for 30 min (Ab) and largely diminished after blocking the antibody with the immunizing peptide (Ab+P). In nonreducing conditions, however, only one prominent and consistent peptide-blockable band was labeled, at ~66 kDa, that exhibited similar density after heating at 65°C for 15 min or 37°C for 30 min. A single 66-kDa protein band in nonreducing conditions was clearly stronger than the 66- and 40-kDa bands in reducing conditions, suggesting the reducing conditions as possibly favorable for splitting the 66-kDa holoprotein in two (or more) fragments, one that retained the antibody-binding epitope (40-kDa protein band) and one or more without it (not labeled on the blot). In addition, a weak ~95-kDa band was inconsistently labeled in various blots that was blocked by the immunizing peptide (Fig. 2*A*) but exhibited no clear relevance to blotting

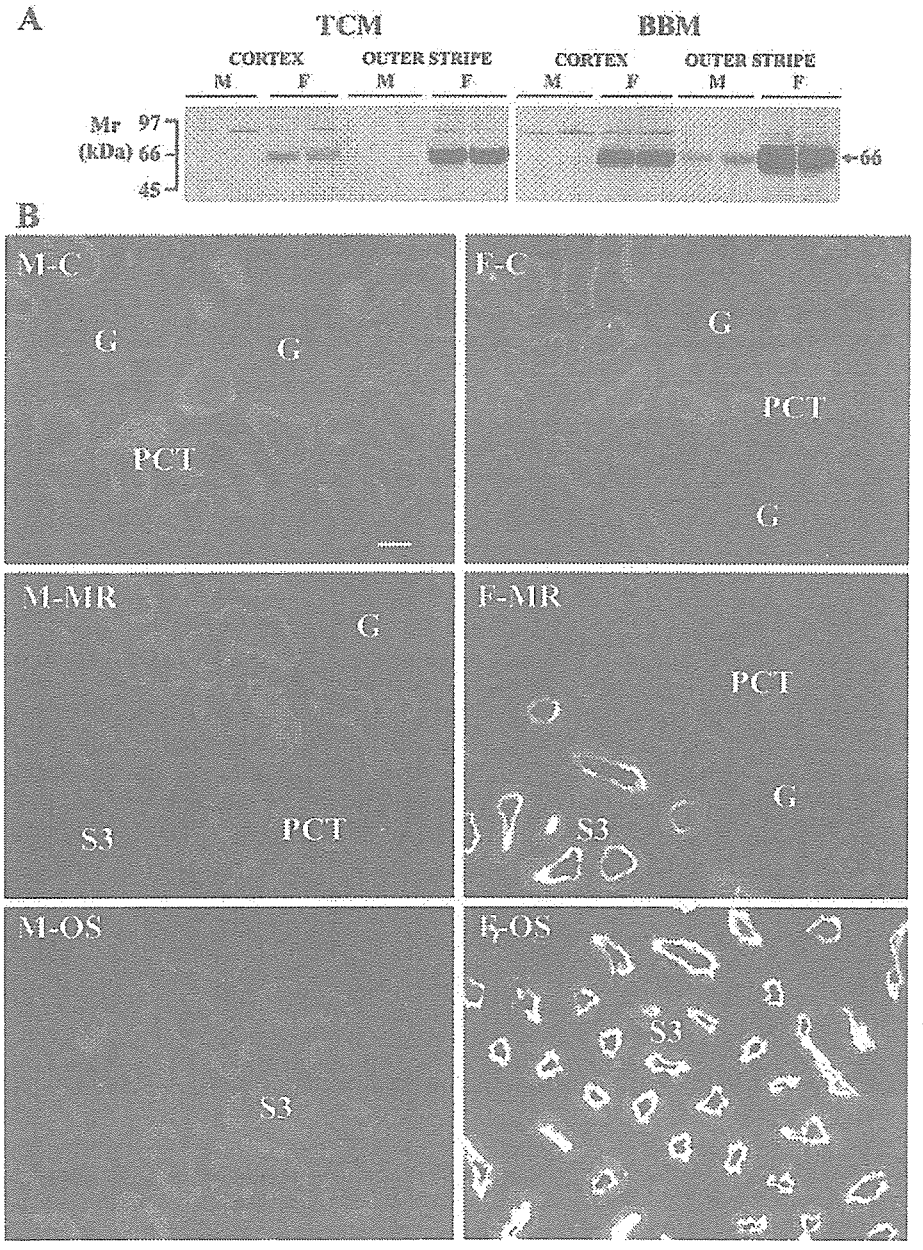

Fig. 3. Zonal and gender differences in the expression of rOAT2 protein in isolated membranes from the cortical and outer stripe tissues (*A*) and in cryosections of the same tissues from the rat kidney (*B*). *A*: comparison of the 66-kDa band in total cell membranes (TCM) and brush-border membranes (BBM) isolated from the cortex (C) and outer stripe (OS). In the membranes from M kidney, the 66-kDa band was either negative or weakly labeled (OS > C), whereas in the membranes from F kidney, the band was labeled in both zones, being much stronger in the OS. Blots were performed with 60 μg (TCM) and 30 μg (BBM) protein/lane. *B*: no significant immunostaining was observed in cryosections of the M kidney superficial cortex (M-C), medullary rays (M-MR), and outer stripe (M-OS), whereas in the F kidney, tubules in the superficial cortex were negative (F-C), but the brush border of proximal tubule S3 segment (S3) in medullary rays (F-MR) and outer stripe (F-OS) was brightly stained. Glomeruli (G) and proximal convoluted tubules (PCT) were negative. Bar = 20 μm.

conditions (Fig. 2*A*), gender (Fig. 3*A*), gonadectomy (Fig. 4*A*), or hormonal treatment (Fig. 6*A*), thus reflecting an OAT2-irrelevant protein that was present in membrane preparations as a variable contamination and was, therefore, neglected. In tissue cryosections, using the optimal experimental conditions and the steps of antigen retrieval, the antibody strongly stained the brush border of proximal tubule S3 segments in the F rat kidney (Fig. 2*B*, Ab). This staining was completely blocked by the immunizing peptide (Fig. 2*B*, Ab+P). In further immunoblotting studies, the membranes were prepared in nonreducing conditions at 37°C for 30 min, whereas the antigen retrieval technique was applied to screen localization of OAT2 in tissue cryosections.

Zonal and gender differences in the expression of OAT2 protein in rat kidney. As shown in Fig. 3*A*, TCM from the M kidney cortex exhibited no significant 66-kDa band, whereas in BBM, the band was either negative (cortex) or weak (outer stripe). No significant band was observed in TCM from the inner stripe and inner medulla (data not shown). Accordingly, in cryosections of the M kidney, either no significant staining with the rOAT2-Ab was observed in any of the structures in the cortex and outer stripe (Fig. 3*B*) or a weak brush-border staining was present in the occasional S3 segments in the outer stripe in some sections (c.f. Fig. 4*C*). However, in TCM and BBM from the F kidney cortex and outer stripe, the 66-kDa band was clearly labeled, showing strong zonal differences

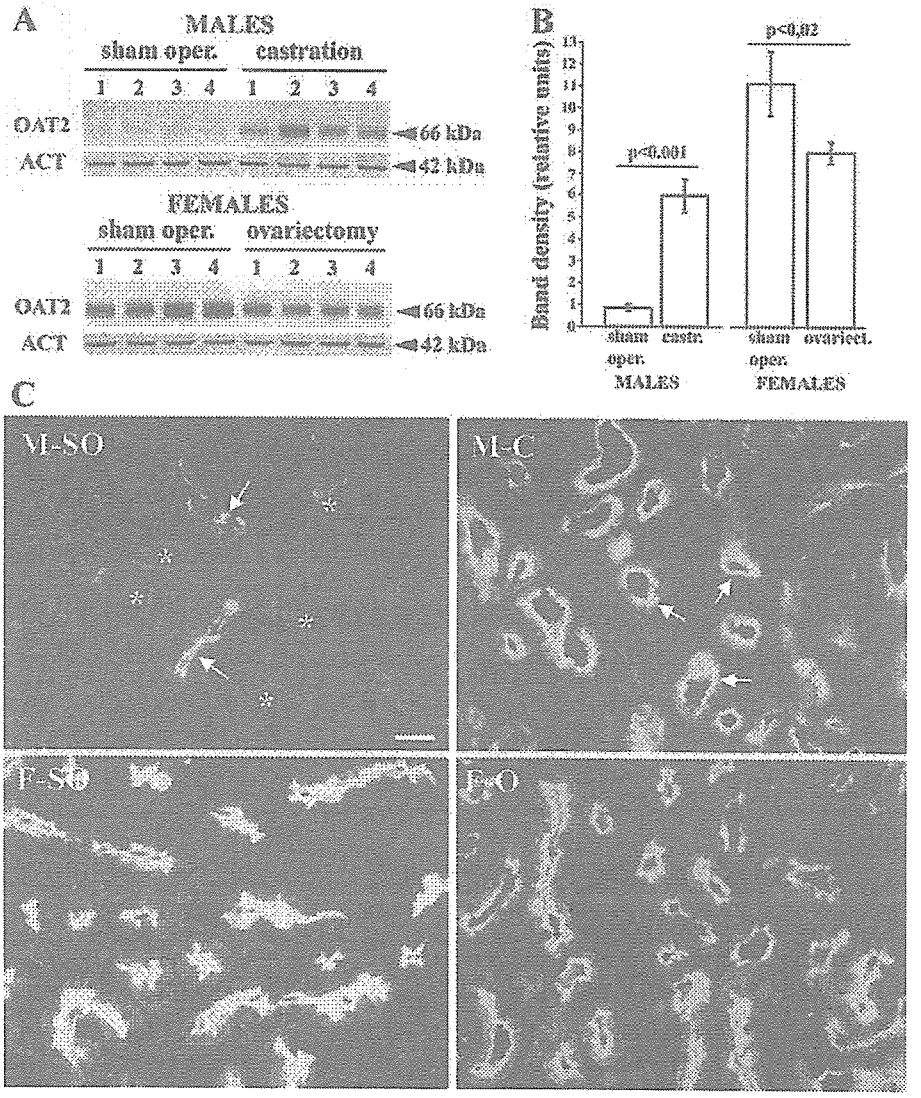

Fig. 4. Effect of castration and ovariectomy on the expression of OAT2 (*A* and *B*) and α-actin (*A*; ACT) in total cell membranes isolated from the outer stripe and OAT2 in cryosections of the same zone of the rat kidney (*C*). *A*: in M rats, the membranes from castrated animals exhibited a much stronger 66-kDa band compared with sham-operated controls, whereas in F rats, the band was weaker in ovariectomized animals compared with controls. The 42-kDa band of α-actin was similar in all the membrane preparations and remained unaffected by gonadectomy. Each band represents membranes from a separate animal. Each lane contained 80 μg of protein. *B*: densitometric evaluation (mean ± SE: $n = 4$ for each experimental group) of the 66-kDa bands shown by immunoblots in *A*. The castrated M exhibited an ~6-fold increase in band density, and the sham-operated F had ~11-fold stronger band density compared with the sham-operated M, whereas the ovariectomized F had ~28% lower band density compared with the respective sham-operated F. *C*: immunostaining of rOAT2 in the inner stripe of sham-operated and gonadectomized rats. In sham-operated M (M-SO), most of the S3 segments were negative (asterisks), and the occasional tubules were weakly apically positive (arrows), whereas the brush border of castrated animals (M-C) was stained much stronger. In sham-operated F (F-SO), the brush border of all S3 segments was brightly stained; the staining intensity was weaker in ovariectomized animals (F-O). Bar = 20 μm.

(outer stripe > cortex) (Fig. 3*A*). The band was absent in TCM from the inner stripe and inner medulla (data not shown). By immunocytochemistry, the staining in F kidney was negative in the superficial cortex, whereas the brush border of S3 segments in the medullary rays and outer stripe was brightly stained (Fig. 3*B*). No significant staining was observed in the inner stripe and inner medulla of M and F kidneys (data not shown). This experiment, therefore, indicates gender (F > M) and zonal (outer stripe > cortex) differences in the expression of OAT2 protein in rat kidney due to an exclusive presence of this transporter in the brush border of proximal tubule S3 segments.

To determine the sex hormone(s) responsible for the observed zonal and gender differences in the expression of OAT2 protein in rat kidney, animals from both sexes were gonadectomized, and castrated M were treated with various sex hormones before immunoblotting and immunocytochemical studies. Because of the exclusive localization of OAT2 in S3 segments, the following data are shown only for isolated membranes and the tissues from the outer stripe.

Effect of castration and ovariectomy in rats. As shown in Fig. 4, *A* and *B*, 6 wk following castration, the OAT2-related 66-kDa band in the renal outer stripe TCM from castrated rats exhibited an approximately sixfold increase above that in sham-operated M. The band density in sham-operated F was ~11-fold stronger than in sham-operated M and decreased by ~28% following ovariectomy. The immunostaining of brush border in S3 segments was *1*) weak in sham-operated M, *2*) strongly upregulated in castrated M, *3*) strong in sham-operated F, and *4*) partially downregulated in ovariectomized F (Fig. 4*C*). The 42-kDa α-actin band was tested in the same membranes (Fig. 4*A*, ACT) and showed no visible differences in variously treated animals, indicating similar protein loading and comparable transfer efficiency. This experiment thus indicates that the expression of OAT2 protein in the rat kidney S3 segments is controlled by inhibitory actions of androgens and stimulatory actions of the F sex hormones.

Expression of OAT2 protein in prepubertal rats. The expression of OAT2 protein in the outer stripe was tested in 20- to

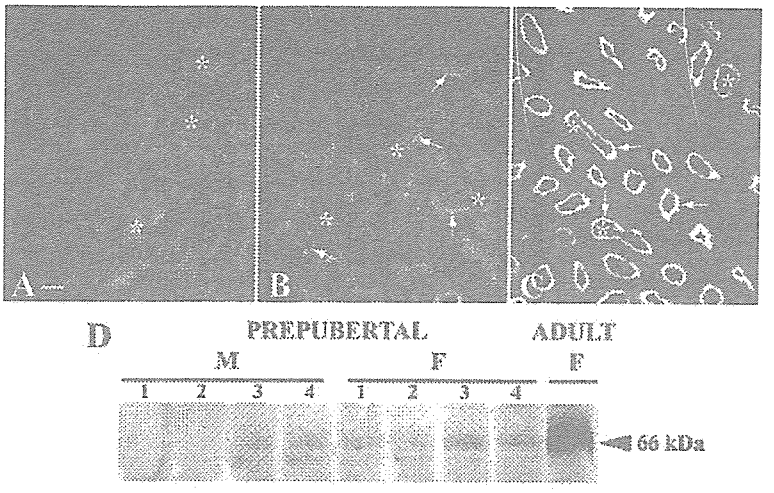

Fig. 5. Expression of rOAT2 protein in the kidney outer stripe of prepubertal rats. *A–C*: immunostaining in the renal outer stripe. In prepubertal rats, the brush-border staining in S3 segments (asterisks) was negative in M (*A*) and very weak in F (*B*, arrows) and comparatively very strong in the adult F (*C*, arrows). Bar = 20 μm. *D*: immunoblotting of rOAT2 in the renal outer stripe total cell membranes from prepubertal M (PPM) and F (PPF) and from an adult F (AF). Compared with that in the adult animal, the rOAT2-related protein band was very weak in prepubertal animals of both sexes. Each lane contained 80 μg of protein and represents membranes from a separate animal.

25-day-old rats of both sexes; as shown in Fig. 5, *A* and *B*, no significant staining with rOAT2-Ab in M rats (Fig. 5*A*) and a very weak staining in F rats (Fig. 5*B*) were observed in the brush-border domain of S3 segments. This pattern of protein expression was confirmed by immunoblotting of TCM isolated from the outer stripe tissue (Fig. 5*D*). The experiment shows that the OAT2 protein expression in rat kidney is very low before the onset of puberty, thus indicating that the observed zonal and gender differences in the OAT2 protein expression in adult animals are related to the levels of sex hormones after puberty.

Effect of sex hormone treatment in castrated rats. To determine the sex hormone responsible for zonal and gender differences in OAT2 expression in adult animals, castrated rats were treated with either oil (control) or various sex hormones (Fig. 6). The immunoblotting data in TCM from the outer stripe of variously treated animals (Fig. 6*A*) and densitometric data of the respective 66-kDa band (Fig. 6*B*) showed that testosterone treatment caused a strong decrease of the elevated band density in castrated rats to the levels observed in sham-operated, oil-treated animals, whereas estradiol and progesterone treatment caused a limited additional upregulation of the band density. The 42-kDa α-actin band in the same membranes (Fig. 6*A*) showed no visible differences in variously treated animals, indicating similar protein loading and comparable transfer efficiency. The immunocytochemical data for OAT2 were completely corroborating (Fig. 6*C*); in accordance with the data in Fig. 4, the staining was largely negative in the outer stripe of sham-operated animals and was clearly enhanced in oil-treated castrated rats. However, testosterone treatment strongly diminished, whereas estradiol and progesterone treatment partially enhanced the brush-border staining in S3 segments of castrated rats. This set of experiments thus indicates that androgens downregulate, whereas estrogens and progesterone upregulate, expression of OAT2 protein in the brush border of S3 segments in rats.

Specificity of rOAT2-Ab in immunoblotting and immunocytochemical studies with the samples from mouse kidney. Previous mRNA studies in mice indicated very low expression of mOAT2 in liver and kidney of the fetal and prepubertal animals (8, 39), and possible gender differences in its expression in liver (F > M) but not in kidney (8, 27) of the adult animals. The amino acid sequence of the rOAT2-immunizing peptide, which is common to both rOAT2 and mOAT2, indicated that the rOAT2-Ab could cross-react with mouse tissues. Indeed, as shown by immunoblotting in TCM and BBM isolated from the whole F mouse kidney, the rOAT2-Ab labeled a single peptide-blockable band at 66 kDa (Fig. 7*A*), whereas by immunocytochemistry, the antibody strongly stained the brush-border domain of proximal tubule S3 segments in the F kidney outer stripe (Fig. 7*B*). This staining was blocked after preincubating the antibody with the immunizing peptide (Fig. 7*C*). The experiments indicate that the rOAT2-Ab cross-reacts with the mOAT2 and was further used for testing the localization of OAT2 protein in the mouse kidney.

Zonal and gender differences in the expression of OAT2 protein in mouse kidney. As shown in Fig. 8, *A–D*, zonal and gender differences in the expression of OAT2 protein are visible by immunostaining cryosections of the mouse kidney. In the M mouse kidney, cortical tubules and other structures exhibited no significant staining (Fig. 8*A*), whereas the brush-border of proximal tubule S3 segments in the outer stripe was weakly stained (Fig. 8*C*). In the cortex of F mouse kidney, only the brush border of S3 segments in medullary rays was fragmentary and weakly stained (Fig. 8*B*), whereas the brush border of S3 segments in the outer stripe was brightly stained (Fig. 8*D*). In immunoblots of the whole mouse kidney BBM, the protein bands related to Na-K-ATPase and AQP1 were similar in both sexes (Fig. 8*E*), whereas the mOAT2-related 66-kDa band was much stronger (~10-fold) in membranes from the F kidneys (Fig. 8, *E* and *F*). Therefore, this set of experiments shows that the expression of OAT2 in mouse kidney exhibits zonal (outer stripe > cortex) and gender differences (F > M) similar to those in rat kidney.

DISCUSSION

The data shown in this report, which were obtained with RT-PCR, Western blotting, and immunocytochemistry, revealed a complete congruency in the expression of renal OAT2-specific mRNA and protein in rats, exhibiting *1*) zonal (outer stripe > cortex) and gender (F > M) differences, *2*)

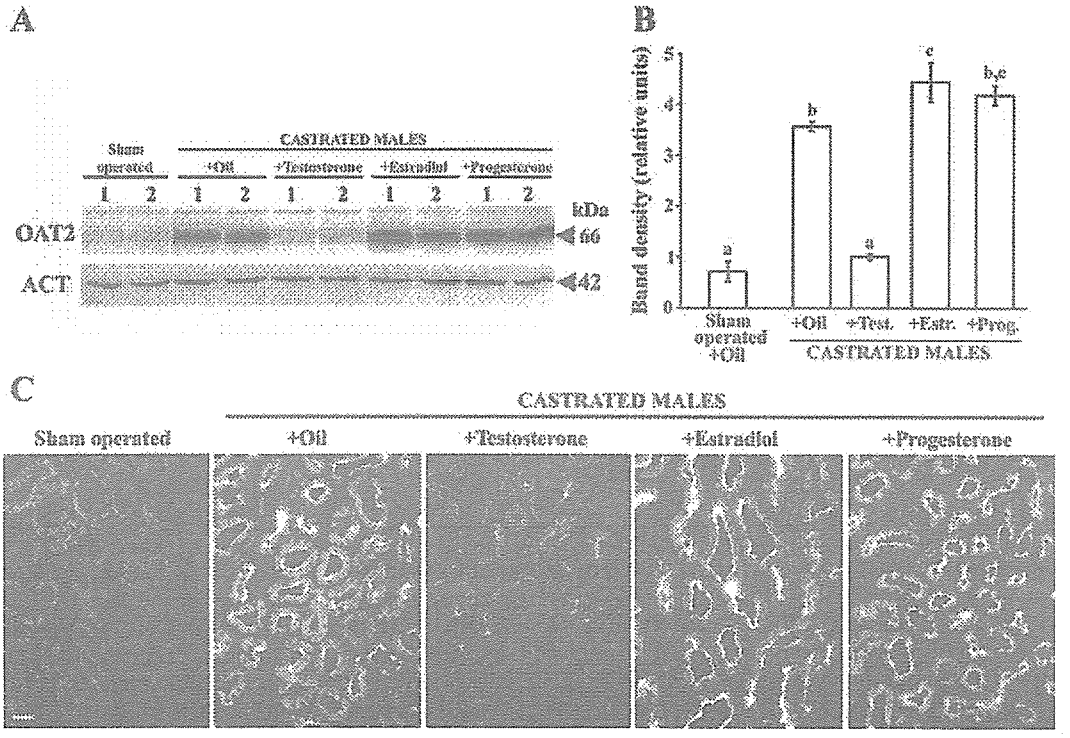

Fig. 6. A representative immunoblot of rOAT2 and α-actin (ACT) with the total cell membranes (each lane contained 80 μg of protein) from the kidney outer stripe (*A*), densitometric evaluation of the rOAT2-related 66-kDa protein band in the blot (*B*), and the respective immunostaining in tissue cryosections (*C*); effect of castration and treatment with various sex hormones in M. *A*: representative blots with membranes from 2 animals in each experimental group. The 42-kDa actin band exhibited no visible differences among various animals, indicating similar loading and transfer. *B*: densitometric data of the 66-kDa band, collected from 2 independent experiments ($n = 4$ in each experimental group); compared with that in sham-operated controls (Sham operated + oil), the density of the 66-kDa protein band was strongly enhanced (~4.5-fold) in castrated rats treated with oil (+Oil); this elevation was downregulated by testosterone treatment to the level of sham-operated animals (+Test), whereas the estradiol (+Estr) or progesterone (+Prog) treatment caused, respectively, an additional significant or limited upregulation vs. oil-treated castrated animals. Statistics: a vs. b or c, $P < 0.001$; b vs. c, $P < 0.05$; other relations, nonsignificant (NS). *C*: immunocytochemically, S3 segments were not stained in the sham-operated + oil-treated rats. BBM of the oil-treated castrated rats was brightly stained, and this staining was strongly diminished after treating animals with testosterone, whereas the staining intensity in estradiol- or progesterone-treated castrated animals was slightly enhanced. Bar = 20 μm.

localization in the brush border of proximal tubule S3 segments (F > M), *3*) weak and gender-independent expression in prepubertal animals, and *4*) similar pattern following gonadectomy and treatment with sex hormones. In addition, the OAT2 protein in mice kidneys exhibited a pattern of localization and gender differences that largely resembled that in rats.

The data of OAT2 mRNA expression in rat kidney, with clear gender differences (F > M), upregulation by castration and downregulation by ovariectomy, as well as downregulation by testosterone and upregulation by estradiol and progesterone treatment in castrated M rats, are in fair agreement with most previously published findings (6, 7, 24, 29). These findings were further corroborated with the immunoblotting data in cell membranes isolated from various kidney zones in rats, showing a comparable gender- and sex hormone-dependent pattern of the rOAT2 protein content. rOAT2 was identified as a temperature- and denaturing condition-sensitive protein exhibiting slightly lower electrophoretic mobility (~66 kDa) than previously observed for the protein in rat liver (52–62 kDa) (36, 50) and kidney (60 kDa) (28). Having 535 amino acid residues (50), the native protein in nonglycosylated state should run to ~59 kDa; the observed location of the band at 66 kDa most probably reflected the glycosylated form of the protein. The pattern of 66-kDa band density in isolated membranes from the renal outer stripe of M, F, and variously treated castrated M rats completely matched the pattern of mRNA expression in the same tissue. Moreover, our immunocytochemical studies revealed *1*) localization of the protein exclusively in the brush border of proximal tubule S3 segments that reside in the outer stripe and in medullary rays and *2*) a pattern of the staining intensity of the brush border in S3 segments comparable to that of mRNA expression and the 66-kDa band density. Taken together, our data showed a missing correlation of the renal OAT2 expression at the levels of mRNA and protein and revealed BBM of the proximal tubule S3 segment as the principal localization of the OAT2 protein in the rat nephron, which is different from the previously attributed localization to the apical membrane of TALH and cortical and medullary collecting ducts in the rat kidney (28). Furthermore, finding of the weak and gender-independent expression of the renal OAT2 protein in prepubertal rats is completely in agreement with previous data showing low mRNA expression in rats under the age of 35 days (6, 50).

In mice, previous studies of the renal OAT2 mRNA indicated its low expression in fetal and prepubertal age and absence of gender differences in adult animals (8, 27, 39). In

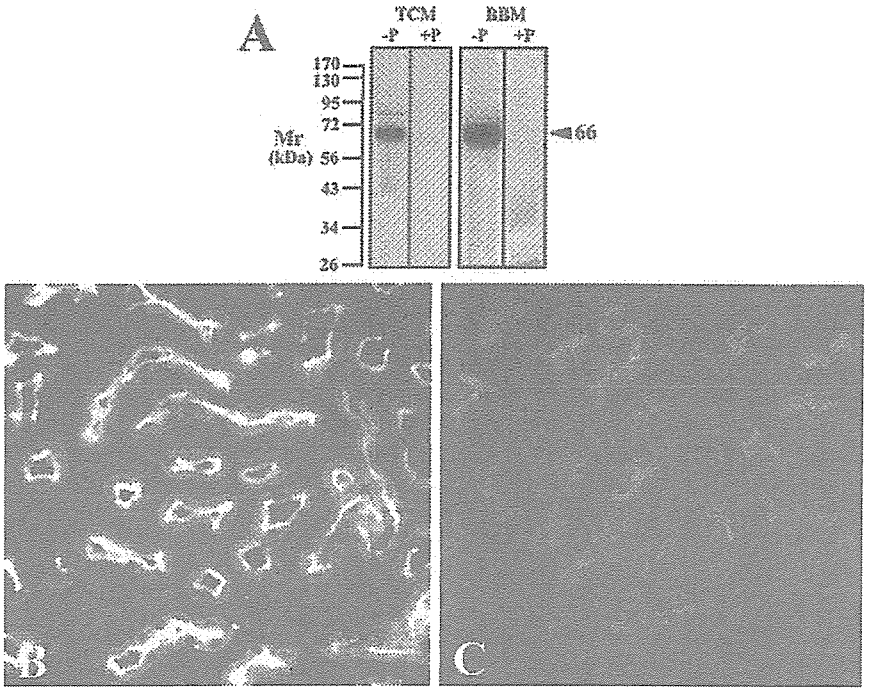

Fig. 7. Testing of rOAT2-Ab specificity by immunoblotting (*A*) and immunocytochemistry (*B* and *C*) in the samples from mouse kidney. *A*: TCM (60 μg protein/lane) and BBM (30 μg protein/lane), isolated from the total F kidney homogenate, were prepared in nonreducing conditions (heating for 15 min at 65°C) and blotted with the rOAT2-Ab (−P) or with the antibody that had been preincubated with the immunizing peptide (+P). In both cases, only 1 significant band of ~66 kDa was labeled that was completely blocked by the peptide. By immunocytochemistry, the brush border of proximal tubule S3 segments in the outer stripe was brightly stained (*B*), and this staining was largely blocked by the immunizing peptide (*C*).

paraffin sections of the M mouse kidney, mOAT2 was recently localized to the luminal membrane of proximal tubules (the segments were not identified) (25). Our data showed that the pattern of localization and gender-dependent expression of OAT2 protein in the mouse proximal tubule S3 segments is basically similar to that in rats, except the staining in M mice was always weakly positive as opposed to the relevant staining in M rats, which was largely negative, whereas the staining in F was strong in both species. The reason for a discrepancy in the expression of renal OAT2 mRNA and protein in mice is unknown and indicates possible sex hormone-dependent post-transcriptional regulation of the OAT2 protein expression in mice, whereas in rats, this regulation seems to be principally transcriptional.

Contrary to the localization of OAT2 in the brush border of S3 segments in rats and mice, the transporter in the human kidney (hOAT2) was immunolocalized to the basolateral membrane of cortical proximal convoluted tubules (13), but possible gender differences in its mRNA and/or protein expression/localization have not been reported. The hOAT2 isoforms (hOAT2A and hOAT2B) are slightly longer than rOAT2 at the COOH-terminal domain, having 546 (hOAT2A) and 538 (hOAT2B) amino acid residues; the isoform hOAT2A exhibits 79% homology to rOAT2 (51). It is unknown whether different COOH-terminal domains represent any discriminating factor for completely different intracellular segregation and targeting of OAT2 to the brush-border (rOAT2 and mOAT2) or basolateral (hOAT2) membrane domains.

The (patho)physiological and possible toxicological implications of the exclusive OAT2 localization in the BBM of S3 segments and its much stronger expression in F rats and mice, as demonstrated in this study, are not clear. Information on the substrate specificity of OAT2 in the mammalian liver and kidney is limited and indicates some differences and similarities among species when studied in the in vitro expression systems: rOAT2 does, but hOAT2 and mOAT2 do not, transport salicylate (27, 48, 51), whereas both rOAT2 and hOAT2 transport some prostaglandins, cephalosporin antibiotics, and other chemotherapeutics (13, 22, 36). Much less is known on the role and substrate specificity of OAT2 in the kidney of experimental animals and humans in vivo, particularly with respect to localization of the transporter in the opposite cell membrane domains. Because of unknown driving forces and nonselective substrate specificity, it is also hard to define a role(s) of the apical and basolateral OAT2 in reabsorptive and/or secretory processes.

The sex-related differences in pharmacokinetics and pharmacodynamics of various exogenous drugs and toxic substances have been documented in animal and human kidney, liver, intestine, and brains (reviewed in Refs. 15, 17, 33, 35, 37). In human and veterinary medicine, these differences may affect the rate of reabsorption, secretion, and therapeutic efficiency and cause adverse reactions to and organotoxicity of various drugs. Numerous information has been collected over the past decade indicating various specific membrane-bound transporters of OA and cations as the critical players in these processes (reviewed in Refs. 4, 12, 14, 18, 19, 31, 35, 37, 38, 40, 52, 53–57). One classic example is the well-studied excretion of PAH in the rat kidney, which is strongly gender dependent (M > F) (3, 23, 41) because of corresponding gender differences in the expression of PAH transporters OAT1 (Slc22a6) and OAT3 (Slc22a8) in the proximal tubule basolateral membrane (M > F) that are caused by androgen stimulation and estrogen inhibition (32). A number of other diagnostic and therapeutic and other potentially toxic but structurally unrelated organic substances have been described whose renal clearance (urine excretion) in rats was gender related, such as aldose reductase inhibitor zenarestat, tauro-

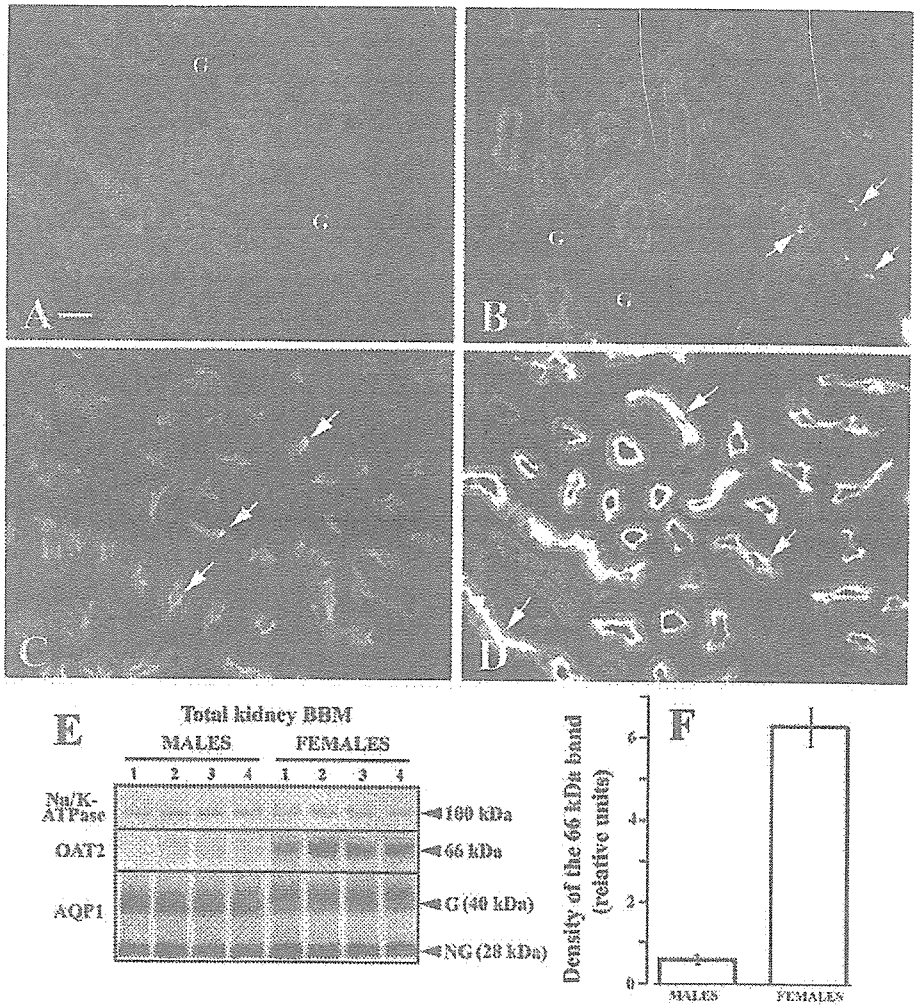

Fig. 8. Zonal and gender differences in the expression of OAT2 protein in cryosections of the mouse kidney (*A–D*), the abundance of Na-K-ATPase, OAT2 and aquaporin-1 (AQP1) in BBM isolated from the whole mouse kidney homogenates (*E*), and densitometric evaluation of the OAT2-related 66-kDa protein (*F*). By immunocytochemistry, in the M kidney, none of the tubule profile was stained in the cortex (*A*), whereas brush border of the proximal tubule S3 segments in the outer stripe was weakly stained (*C*, arrows). In the F kidney, most of the tubules in the cortex were not stained, except for S3 segments in the medullary rays, whose brush border was fragmentary and weakly stained (*B*, arrows), whereas brush border of the S3 segments in the outer stripe was strongly stained (*D*, arrows). G, glomeruli. Bar = 20 μm. In immunoblots of the total kidney BBM (*E*), the abundances of Na-K-ATPase (~100-kDa band of the α-subunit) and AQP1 (nonglycosylated 28-kDa and glycosylated ~40-kDa bands) were similar in membrane preparations from both sexes, indicating similar quality of isolated membranes, whereas the OAT2-related 66-kDa band was much stronger in membranes from the F kidneys. Each lane contained 30 μg of protein. Densitometric evaluation of the 66-kDa band (*F*) exhibited ~10-fold higher abundance of this protein in F animals (n = 4 in each experimental group, $P < 0.001$).

cholate and dibromosulfophtalein (F > M) (21, 54), estradiol-17β-glucuronide (F > M) (16), anti-ulcer drug egualen sodium (F > M) (45), semisynthetic penicillin metabolite cyclacillin (F > M) (20), and 2-butoxyethanol (M > F) (11). Whereas gender-dependent excretion of zenarestat, taurocholate, and dibromosulfophtalein may be related to the renal expression of OA-transporting polypeptide-1 (OATP1/Slc21a1) in the brush border of proximal tubule S3 segments, which is stimulated by androgens at both the mRNA and protein levels (34) and thus may mediate much higher reabsorption of these substrates in M rats (21, 16), gender differences in the excretion of other above-mentioned substances have not been correlated to any specific transporter so far.

As a transporter for cyclosporin antibiotics, OAT2 may contribute to a well-known nephrotoxicity by these compounds in humans (22), but information regarding possible gender differences of the hOAT2 in the proximal tubule basolateral membrane and nephrotoxicity are not available. On the other side, sex hormone-driven gender differences in the expression of rOAT2 protein in the brush border of proximal tubule S3 segments in rats (this study) are in fair correlation with the OAT2 mRNA expression and renal excretion of an occupational toxicant, perfluorooctanoic acid (PFOA), whose clearance is much lower in M rats, increased by castration, and decreased strongly by testosterone and weakly by estradiol treatment in castrated animals (29). This putative correlation, "substrate clearance-rOAT2 expression," implies that the transporter would act in secretory mode and would transport less PFOA in M. However, a number of other OA transporters exist at the basolateral or BBM domains in proximal tubules whose driving forces are only partially or ill defined, with a wide substrate specificity and undefined reabsorptive or secretory mode of action in vivo, and a number of them may exhibit gender differences that could interfere with the PFOA excretion.

In summary, our study indicates that the rat renal OAT2 is localized exclusively in the brush border of proximal tubule S3 segments, causing zonal (outer stripe > cortex) and gender differences (F > M) in both mRNA and protein expression that are determined by androgen inhibition and estrogen and progesterone stimulation, and appear after puberty. A similar gender-dependent pattern of OAT2 expression also exists in the mouse kidney. The impact of these findings on gender- and age-related reabsorption, secretion, and nephrotoxicity of endogenous and exogenous OA in rodents should be defined in future studies. Furthermore, keeping in mind the different

localization of the OAT2 protein in rodents (BBM of the proximal tubule S3 segment) and humans (basolateral membrane of the proximal tubules), it is unclear whether rodents can serve as a plausible model for humans with regard to the proposed role of OAT2 in renal physiology and nephrotoxicity, so that further experimentation is urged to resolve species differences in the OAT2 expression and function(s).

ACKNOWLEDGMENTS

We thank the company Transgenic, Incorporated (Kumamoto, Japan), for providing the anti-rOAT2 antibody and Mrs. Eva Heršak for expert technical assistance.

GRANTS

This work was supported by Grant no. 0022011 (I. Sabolić) from the Ministry for Science, Education and Sports, Republic of Croatia.

REFERENCES

1. **Biber J, Stieger B, Haase W, Murer H.** A high yield preparation for rat kidney brush-border membranes: different behavior of lysosomal markers. *Biochim Biophys Acta* 647: 169–176, 1981.
2. **Bradford MM.** A rapid and sensitive method for the quantitation of microgram quantities of protein utilizing the principle of protein-dye binding. *Anal Biochem* 72: 248–254, 1976.
3. **Braunlich H, Meinig T, Grosch U.** Postnatal development of sex differences in renal tubular transport of *p*-aminohyppurate (PAH) in rats. *Exp Toxicol Pathol* 45: 309–313, 1993.
4. **Bridges CC, Zalups RK.** Molecular and ionic mimicry and the transport of toxic metals. *Toxicol Appl Pharmacol* 204: 274–308, 2005.
5. **Brown D, Lydon J, McLaughlin M, Stuart A, Tyszkowsky R, Alper S.** Antigen retrieval in cryostat sections and cultured cells by treatment with sodium dodecyl sulfate (SDS). *Histochem Cell Biol* 105: 261–267, 1996.
6. **Buist SCN, Cherrington NJ, Choudhuri S, Hartley DP, Klaassen CD.** Gender-specific and developmental influences on the expression of rat organic anion transporters. *J Pharmacol Exp Ther* 301: 145–151, 2002.
7. **Buist SCN, Cherrington NJ, Klaassen CD.** Endocrine regulation of rat organic anion transporters. *Drug Metab Dispos* 31: 559–564, 2003.
8. **Buist SCN, Klaassen CD.** Rat and mouse differences in gender-predominant expression of organic anion transporter (OAT1–3; SLC22A6–8) mRNA levels. *Drug Metab Dispos* 32: 620–625, 2004.
9. **Burckhardt BC, Burckhardt G.** Transport of organic anions across the basolateral membrane of proximal tubule cells. *Rev Physiol Biochem Pharmacol* 146: 95–158, 2003.
10. **Cerrutti JA, Brandoni A, Quaglia NB, Torres AM.** Sex differences in p-aminohippuric acid transport in rat kidney: role of membrane fluidity and expression of OAT1. *Mol Cell Biochem* 233: 175–179, 2002.
11. **Dill JA, Lee KM, Bates DJ, Anderson DJ, Johnson RE, Chou BJ, Burka LT, Roycroft JH.** Toxicokinetics of inhaled 2-butoxyethanol and its major metabolite, 2-butoxyacetic acid, in F344 rats and B6C3F1 mice. *Toxicol Appl Pharmacol* 153: 227–242, 1998.
12. **Endou H.** Recent advances in molecular mechanisms of nephrotoxicity. *Toxicol Lett* 102–103: 29–33, 1998.
13. **Enomoto A, Takeda M, Shimoda M, Narikawa S, Kobayashi Y, Kobayashi Y, Yamamoto T, Sekine T, Cha SH, Niwa T, Endou H.** Interaction of human organic anion transporters 2 and 4 with organic anion transport inhibitors. *J Pharmacol Exp Ther* 301: 797–802, 2002.
14. **Eraly SA, Blantz RC, Bhatnagar V, Nigam SK.** Novel aspects of renal organic anion transporters. *Curr Opin Nephrol Hypertens* 12: 551–558, 2003.
15. **Fletcher CV, Acosta EP, Strykowski JM.** Gender differences in human pharmacokinetics and pharamacodynamics. *J Adolesc Health* 15: 619–629, 1994.
16. **Gotoh Y, Kato Y, Stieger B, Meier PJ, Sugiyama Y.** Gender differences in the Oatp1-mediated tubular reabsorption of estradiol-17beta-D-glucuronide in rats. *Am J Physiol Endocrinol Metab* 282: E1245–E1254, 2002.
17. **Harris RZ, Benet LZ, Schwartz JB.** Gender effects in pharmacokinetics and pharamacodynamics. *Drugs* 50: 222–239, 1995.
18. **Ho RH, Kim RB.** Transporters and drug therapy: implications for drug disposition and disease. *Clin Pharmacol Ther* 78: 260–277, 2005.
19. **Inui K, Masuda S, Saito H.** Cellular and molecular aspects of drug transport in the kidney. *Kidney Int* 58: 944–958, 2000.
20. **Janssen FW, Young EM, Ruelius HW.** Effect of sex hormones on the disposition in rats of 1-aminocyclohexane carbocyclic acid, a metabolite of semisynthetic penicillin. *Drug Metab Dispos* 4: 540–546, 1976.
21. **Kato Y, Kuge H, Kusuhara H, Meier PJ, Sugiyama Y.** Gender differences in the urinary excretion of organic anions in rats. *J Pharmacol Exp Ther* 302: 483–489, 2002.
22. **Khamdang S, Takeda M, Babu E, Noshiro R, Onozato ML, Tojo A, Enomoto A, Huang XL, Narikawa S, Anzai N, Piyachaturawat P, Endou H.** Interaction of human and rat anion transporter 2 with various cephalosporin antibiotics. *Eur J Pharmacol* 465: 1–7. 2003.
23. **Kleinman LI, Loewenstein MS, Goldstein L.** Sex difference in the transport of *p*-aminohyppurate by the rat kidney. *Endocrinology* 78: 403–406, 1966.
24. **Kobayashi N, Hirokawa N, Ohshiro N, Sekine T, Sasaki T, Tokuyama S, Endou H, Wamamoto T.** Differential gene expression of organic anion transporters in male and female rats. *Biochem Biophys Res Commun* 290: 482–487, 2002.
25. **Kobayashi Y, Ohbayashi M, Kohyama N, Yamamoto T.** Mouse organic anion transporter 2 and 3 (mOAT2/3 [Slc22a7/8]) mediates the renal transport of bumetanide. *Eur J Pharmacol* 524: 44–48, 2005.
26. **Kobayashi Y, Ohshiro N, Sakai R, Ohbayashi M, Kohyama N, Yamamoto T.** Transport mechanism and substrate specificity of human organic anion transporter 2 (hOAT2/SLC22A7). *J Pharm Pharmacol* 57: 573–578, 2005.
27. **Kobayashi Y, Ohshiro N, Shibusawa A, Sasaki T, Tokuyama S, Sekine T, Endou H, Yamamoto T.** Isolation, characterization and differential gene expression of multispecific organic anion transporter 2 in mice. *Mol Pharmacol* 62: 7–14, 2002.
28. **Kojima R, Sekine T, Kawachi M, Cha SH, Suzuki Y, Endou H.** Immunolocalization of multispecific organic anion transporters, OAT1, OAT2, and OAT3, in rat kidney. *J Am Soc Nephrol* 13: 848–857, 2002.
29. **Kudo N, Katakura M, Sato Y, Kawashima Y.** Sex hormone-regulated renal transport of perfluorooctanoic acid. *Chem Biol Interact* 139: 301–316, 2002.
30. **Kusuhara H, Sekine T, Utsunomiya-Tate N, Tsuda M, Kojima R, Cha SH, Sugiyama Y, Kanai Y, Endou H.** Molecular cloning and characterization of a new multispecific organic anion transporter from rat brain. *J Biol Chem* 274: 13675–13680, 1999.
31. **Lee W, Kim RB.** Transporters and renal drug elimination. *Annu Rev Pharmacol Toxicol* 44: 137–166, 2004.
32. **Ljubojevic M, Herak-Kramberger CM, Hagos Y, Bahn A, Endou H, Burckhardt G, Sabolic I.** Rat renal cortical OAT1 and OAT3 exhibit gender differences determined by both androgen stimulation and estrogen inhibition. *Am J Physiol Renal Physiol* 287: F124–F138, 2004.
33. **Lohr JW, Willsky GR, Acara MA.** Renal drug metabolism. *Pharmacol Rev* 50: 107–141, 1998.
34. **Lu R, Kanai N, Wolkoff AW, Schuster VL.** Regulation of renal oatp mRNA expression by testosterone. *Am J Physiol Renal Fluid Electrolyte Physiol* 270: F332–F337, 1996.
35. **Mizuno N, Niwa T, Yotsumoto Y, Sugiyama Y.** Impact of drug transporter studies on drug discovery and development. *Pharmacol Rev* 55: 425–461, 2003.
36. **Morita N, Kusuhara H, Sekine T, Endou H, Sugiyama Y.** Functional characterization of rat organic anion transporter 2 in LLC-PK1 cells. *J Pharmacol Exp Ther* 298: 1179–1184, 2001.
37. **Morris ME, Lee HJ, Predko LM.** Gender differences in the membrane transport of endogenous and exogenous compounds. *Pharmacol Rev* 55: 229–240, 2003.
38. **Motohashi H, Sakurai Y, Saito H, Masuda S, Urakami Y, Goto M, Fukatsu A, Ogawa O, Inui K.** Gene expression levels and immunolocalization of organic ion transporters in the human kidney. *J Am Soc Nephrol* 13: 866–874, 2002.
39. **Pavlova A, Sakurai H, Leclercq B, Beier DR, Yu ASL, Nigam SK.** Developmentally regulated expression of organic ion transporters NKT (OAT1), OCT1, NLT (OAT2), and Roct. *Am J Physiol Renal Physiol* 278: F635–F643, 2000.
40. **Pritchard JB, Miller DS.** Mechanisms mediating renal secretion of organic anions and cations. *Physiol Rev* 73: 765–796, 1993.
41. **Reyes JL, Melendez E, Alegria A, Jaramillo-Juarez F.** Influence of sex differences on the renal secretion of organic anions. *Endocrinology* 139: 1581–1587, 1998.
42. **Sabolic I, Herak-Kramberger CM, Antolovic R, Breton S, Brown D.** Loss of basolateral invaginations in proximal tubules of cadmium-intox-

icated rats is independent of microtubules and clathrin. *Toxicology* 218: 149–163, 2006.
43. **Sabolic I, Herak-Kramberger CM, Breton S, Brown D.** Na/K-ATPase in intercalated cells along the rat nephron revealed by antigen retrieval. *J Am Soc Nephrol* 10: 913–922, 1999.
44. **Sabolic I, Valenti G, Verbavatz JM, Van Hoek AN, Verkman AS, Ausiello DA, Brown D.** Localization of the CHIP28 water channel in rat kidney. *Am J Physiol Cell Physiol* 263: C1225–C1233, 1992.
45. **Sato M, Suzaka H, Miyazaki H.** Sex-related differences in urinary excretion of egualen sodium in rats. *Drug Metab Dispos* 28: 21–27. 2000.
46. **Schlattjan JH, Biggermann F, Greven J.** Gender differences in renal tubular taurocholate transport. *Naunyn Schmiedebergs Arch Pharmacol* 371: 449–456, 2005.
47. **Sekine T, Cha SH, Endou H.** The multispecific organic anion transporter (OAT) family. *Pflügers Arch* 440: 337–350, 2000.
48. **Sekine T, Cha SH, Tsuda M, Apiwattanakul N, Nakajima N, Kanai Y, Endou H.** Identification of multispecific organic anion transporter 2 expressed predominantly in the liver. *FEBS Lett* 429: 179–182, 1998.
49. **Sekine T, Miyazaki H, Endou H.** Molecular physiology of renal organic anion transporters. *Am J Physiol Renal Physiol* 290: F251–F261, 2006.
50. **Simonson GD, Vincent AC, Roberg KJ, Huang YE, Iwanij W.** Molecular cloning and characterization of a novel liver-specific transport protein. *J Cell Sci* 107: 1065–1067, 1994.
51. **Sun W, Wu RR, van Poelje PD, Erion MD.** Isolation of a family of organic anion transporters from human liver and kidney. *Biochem Biophys Res Commun* 283: 417–422, 2001.
52. **Sweet DH.** Organic anion transporter (Slc22a) family members as mediators of toxicity. *Toxicol Appl Pharmacol* 204: 198–215, 2005.
53. **Sweet DH, Bush KT, Nigam SK.** The organic anion transporter family: from physiology to ontogeny and the clinic. *Am J Physiol Renal Physiol* 281: F197–F205, 2001.
54. **Tanaka Y, Kadoh Y, Mukumoto S, Ishikawa H.** The role of age and sex hormones on the urinary excretion of zenarestat in rats. *Xenobiotica* 21: 1273–1279, 1991.
55. **Terlouw SA, Masereeuw R, Russel FGM.** Modulatory effects of hormones, drugs, and toxic events on renal organic anion transport. *Biochem Pharmacol* 65: 1393–1405, 2003.
56. **Van Aubel RAMH, Masereeu R, Russel FGM.** Molecular pharmacology of renal organic anion transporters. *Am J Physiol Renal Physiol* 279: F216–F232. 2000.
57. **Wright SH, Dantzler WH.** Molecular and cellular physiology of renal organic cation and anion transport. *Physiol Rev* 84: 987–1049, 2004.

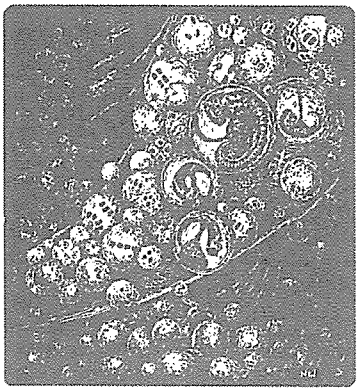

Expression of Rat Renal Cortical OAT1 and OAT3 in Response to Acute Biliary Obstruction

Anabel Brandoni,[1] Silvina R. Villar,[1] Juan C. Picena,[2] Naohiko Anzai,[3] Hitoshi Endou,[3] and Adriana M. Torres[1]

Renal function in the course of obstructive jaundice has been the subject of great interest; however, little is known about the expression of renal organic anion transporters. The objective of this work was to study, in rats with acute extrahepatic cholestasis, the cortical renal expression of the organic anion transporter 1 (OAT1) and the organic anion transporter 3 (OAT3), in association with the pharmacokinetics and renal excretion of furosemide (FS). Male Wistar rats underwent bile duct ligation (BDL rats). Pair-fed sham-operated rats served as controls. All studies were carried out 21 hours after surgery. Rats were anesthetized and the pharmacokinetic parameters of FS and the renal elimination of FS were determined. Afterwards, the kidneys were excised and processed for immunoblot (basolateral membrane and renal homogenates) or immunocytochemical (light microscopic and confocal immunofluorescence microscopic analysis) techniques. The systemic and renal clearance of FS as well as the excreted and secreted load of FS increased in BDL rats. In kidneys from BDL rats, immunoblotting showed a significant increase in the abundance of both OAT1 and OAT3 in homogenates from renal cortex. In basolateral membranes from kidney cortex of BDL rats, OAT1 abundance was also increased and OAT3 abundance was not modified. Immunocytochemical techniques confirmed these results. In conclusion, acute obstructive jaundice is associated with an upregulation of OAT1 and OAT3, which might explain, at least in part, the increased systemic and renal elimination of FS. (HEPATOLOGY 2006;43:1092-1100.)

Obstructive jaundice is defined as retention of bile and bile components after extrahepatic or intrahepatic bile duct obstruction. Extrahepatic cholestasis refers to obstruction of large bile ducts outside the liver, for instance, due to gallstones.[1-4]

Kidney and liver eliminate numerous potentially toxic xenobiotics, including drugs, toxins, and endogenous metabolites. In some cases, the loss of one route of elimination can be compensated for by the other.[5] Limited data are available on the pharmacokinetics of drugs in subjects with biliary obstruction. A number of drugs, such as β-lactam antibiotics, diuretics, nonsteroidal anti-inflammatory drugs, and several antiviral drugs, are classified as organic anions. The tubular secretion of organic anions is an important function of the kidney by eliminating these kinds of drugs from the body.[6] Therefore, the renal organic anion transport system plays a key role in the pharmacokinetics of these drugs.[6]

Several carrier proteins from this transport system have been cloned and functionally characterized from both membrane domains of rat kidneys.[6-8] Organic anion transporter 1 (OAT1) and 3 (OAT3) represent the key organic anions/α-ketoglutarate exchangers in the energetically linked basolateral entry of organic anions into the proximal tubule cells of the kidneys.[9,10] The multidrug resistance protein 2 (MRP2) and the multidrug resistance protein 4 (MRP4) are organic anions carriers located in the apical membranes from proximal tubule cells.[11,12] Tanaka et al.[13] have shown that in bile duct-ligated rats, the expression of MRP2 was upregulated at the transcription level and that the expression of the protein was increased in renal epithelial cells but downregulated in

Abbreviations: OAT, organic anion transporter; MRP, multidrug resistance protein; PAH, p-aminohippurate; FS, furosemide; NKCC2, Na-K-2Cl cotransporter; BDL, bile duct ligation; UENa, urinary excretion rate of sodium; UF, urinary flow; BLM, basolateral membranes; ALP, alkaline phosphatase; HRP, horseradish peroxidase; PAS, periodic acid-Schiff.

From the [1]Farmacología. Facultad de Ciencias Bioquímicas y Farmacéuticas, CONICET; [2]Cátedra de Anatomía y Fisiología Patológicas, Facultad de Ciencias Médicas; Universidad Nacional de Rosario, Argentina; and the [3]Department of Pharmacology and Toxicology, Kyorin University School of Medicine, Tokyo, Japan.

Received October 5, 2005; accepted February 2, 2006.

Support for this study was provided by Agencia Nacional de Promoción Científica y Tecnológica and CONICET. Silvina R. Villar was a recipient of a grant from Fundación Antorchas. Adriana M. Torres was a recipient of a travel grant from CONICET/JSPS (Japan Society for the Promotion of Science).

Address reprint requests to: Adriana M. Torres, Ph.D., Professor of Pharmacology, Suipacha 531, Rosario, 2000 Argentina. E-mail: adtorres@fbioyf.unr.edu.ar; fax: (54) 341-4371992.

Published online in Wiley InterScience (www.interscience.wiley.com).

DOI 10.1002/hep.21142

Potential conflict of interest: Nothing to report.

hepatocytes. Moreover, we have demonstrated an increase in the urinary excretion of p-aminohippurate (PAH) concomitantly with an increase in the abundance of OAT1 in kidney homogenates from rats with extrahepatic cholestasis of 21 hours.[14] This preliminary study showed the modification of OAT1 abundance in kidney homogenates and did not determine the expression of OAT1 in basolateral membranes from kidney cells. The important function of OAT1 in the elimination of organic anions is performed by OAT1 protein units placed in basolateral plasma membranes.

Furosemide (FS) is a well-known organic anion that exerts its diuretic action by binding to the Na-K-2Cl cotransporter (NKCC2) in the thick ascending limb of Henle's loop.[15,16] Because FS is extensively bound to plasma proteins, delivery of this drug to the tubules by filtration is limited. However, it is efficiently secreted by the organic anion's transport system in the proximal tubule and thereby gains access to its binding site. OAT1 and OAT3 are involved in the renal tubular secretion of FS and are thereby responsible for their delivery to the site of action in effective amounts.[17-19]

The purpose of the current study was to examine the effects of acute extrahepatic cholestasis on the expression of OAT1 and OAT3 in rats, and the contribution of these effects on the pharmacokinetics and renal excretion of FS. We chose FS as a prototype of organic anion used to treat a wide variety of therapeutic conditions that can take place simultaneously with extrahepatic cholestasis.

Materials and Methods

Experimental Animals. Male Wistar rats aged from 110 to 130 days were used throughout the study (380-410 g body weight). Animals were anesthetized with sulfuric ether. After an upper abdominal incision performed under sterile technique, the common bile duct was isolated and double-ligated close to the liver hilus immediately below the bifurcation and cut between the ligatures [bile duct ligation (BDL) group]. Controls underwent a sham operation that consisted of exposure, but not ligation, of the common bile duct (sham group). The abdominal incision was then closed by single sutures. All studies were performed 21 hours after surgery. Animals were cared for in accordance with the principles and guidelines for the care and use of laboratory animals, recommended by the National Academy of Sciences and published by the National Institutes of Health (NIH publication 86-23 revised 1985).

Biochemical Determinations. The day of the experiment, blood samples were withdrawn and used to measure total and direct bilirubin as indicative parameters of hepatic function and urea serum levels as an indicative parameter of global renal function. These biochemical analyses were performed employing commercial kits (Wiener Laboratory, Athens, Greece).

Pharmacokinetic Studies. These studies were done similarly to previously described.[20-22] At 21 hours after surgery, sham (n = 5) and BDL (n = 6) rats were anesthetized with sodium thiopental (70 mg/kg body weight, intraperitoneally). A single bolus of FS (10 mg/kg, aqueous solution, intravenously) was administered through a femoral venous catheter. Blood samples from femoral artery were obtained at 0 to 120 minutes after administration of the FS solution. Meanwhile, urine was collected in proper vials, to measure the quantity of FS.

The plasma concentration versus time curves for FS for each individual animal were fitted with the PKCALC computer program.[23] Data were fitted to a bi-exponential curve. The choice of the best fit was based on the determination of coefficient values (R^2) and F test.[23,24] All fits had R^2 values > 0.9.

Concentration of FS in plasma and urine was measured using the method described by Bratton and Marshall.[25]

Renal Excretion Studies. These studies were performed as previously described.[21,26-28] Sham (n = 7) and BDL (n = 7) rats received a priming dose of inulin (30 mg/kg body weight) and FS (5 mg/kg body weight) in 1.5 mL saline solution through a femoral venous catheter. A solution containing inulin (12 g/L), FS (0.9 g/L), and saline solution (9 g/L) was infused by employing a constant infusion pump (Pump 22; Harvard Apparatus, Holliston, MA) at a rate of 1 mL/h/100 g body weight. After equilibrating for 45 minutes, urine was collected during two 20-minute periods, through a bladder catheter. Blood from the femoral artery was obtained at the midpoint of each clearance period. Arterial blood pressure was estimated throughout the experiments with a manometer inserted in the femoral artery. The glomerular filtration rate was calculated from the clearance of inulin. The excreted, secreted, and filtered loads of FS, the urinary excretion rate of sodium (UENa) and the urinary flow (UF) were calculated by conventional formulae for each animal. FS was measured as described previously. Inulin concentrations were assayed by the procedure of Roe.[29] Sodium concentrations in urine were determined by flame photometry and the volume of urine by gravimetry.

Binding of FS to plasma proteins was determined by ultrafiltration as previously described by Cerrutti et al.[21]

Preparation of Basolateral Membranes. The preparations of basolateral membranes (BLM) from sham and BDL rats were done by a modification of the method

described by Jensen and Berndt,[30] as previously reported by us.[21,31] Each preparation represented cortical tissue from four animals. Four different BLM preparations were obtained for each experimental group. The purity of BLM was ascertained through analyses of marker enzymes, Na,K-ATPase for BLM and alkaline phosphatase (ALP) for brush border membranes. Na,K-ATPase activity was estimated as previously described.[21,32-35] ALP was determined using a commercial Kit (Wiener Lab, Argentina). The activity of Na,K-ATPase was enriched in BLM more than eight times relative to that in their respective homogenate (see Results). The enrichment of ALP was approximately 1.5 to 1.9. The ALP activities (mUI/mg protein) were not statistically different both in kidney cortex homogenates (512 ± 86, n = 4 vs. 352 ± 44, n = 4) and in BLM (952 ± 187, n = 4 vs. 541 ± 156, n = 4) from BDL rats as compared with sham rats, respectively. The enrichment and purity of these BLM were comparable to those reported previously[21,34,35] and similar between sham and BDL groups.

Protein quantification of homogenates and BLM was performed using the Sedmak and Grossberg method.[36]

Uptake Studies. Because radiolabeled FS is not commercially available, we measured PAH uptake in BLM vesicles from Sham and BDL rats. PAH, as FS, is also transported by OAT1 and by OAT3 in BLM from rat kidneys.[6-8]

PAH uptake by BLM vesicles was measured by the rapid filtration technique as previously described.[21,34] Briefly, BLM vesicles (150-250 μg protein) were added to an incubation medium containing 100 mmol/L NaCl, 100 mmol/L sucrose, 20 mmol/L Hepes-Tris pH 7.40, 10 μmol/L α-ketoglutarate, and 400 μmol/L ^{3}H-PAH. After 15 seconds, the uptake was terminated by diluting the samples to 1.0 mL with ice-cold stop solution (150 mmol/L KCl, 20 mmol/L Hepes-Tris, pH 7.40).

Electrophoresis and Immunoblotting. Immunoblotting and subsequent densitometry for OAT1 and OAT3 were performed in homogenates and BLM as previously described,[31,35,37,38] using a commercial rabbit polyclonal antibody against rat OAT1 (Alpha Diagnostic International, San Antonio, TX) and a non-commercial rabbit polyclonal antibody against rat OAT3.[39] Blots were processed for detection, using a commercial kit (Opti-4CN, Bio-Rad for OAT1 and ECL enhanced chemiluminescence system, Amersham, Buckinghamshire, UK, for OAT3). Membranes were stained with Ponceau Red to confirm equal protein loading and transfer between lanes as previously described.[14,28,31,37,40]

Immunocytochemistry Microscopy. Kidneys from sham (n = 4) and BDL (n = 4) rats were processed as previously described.[35,38] Kidney sections were incubated with non-commercial polyclonal antibodies against OAT1 (diluted 1:1,000) or OAT3 (diluted 1:1,000) overnight at 4°C. The specificity of both antibodies has been described elsewhere.[39,41]

Light Microscope Analysis. The sections were incubated with biotinylated secondary antibody against rabbit immunoglobulin for 1 hour (biotinylated Ig Multi-Link, Biogenex, San Ramon, CA). They were then incubated for 30 minutes with horseradish peroxidase (HRP)-conjugated streptavidin solution (streptavidin/HRP complex multi-link, Biogenex). To detect HRP labeling, a peroxidase substrate solution with diaminobenzidine (0.05% diaminobenzidine in PBST with 0.05 % H_2O_2) was used. Sections were counterstained with hematoxylin before being examined under a light microscope.

Confocal Microscope Analysis. The sections were incubated with Alexa 488 fluorochrome-conjugated goat anti-rabbit IgG, 1:1000 (Molecular Probes, Eugene, OR) overnight at 4°C and then mounted. Sections were viewed on a Zeiss Axiophot microscope equipped with an epifluorescence detector and a Bio-Rad MRC 1260 confocal imaging system.

Controls using preimmune serum, antiserum absorbed with excess synthetic peptide, or omission of primary or secondary antibody showed no labeling.

Histopathological Studies. Histopathology of kidneys was performed after fixing in 10% neutral buffered formaldehyde solution for 4 hours and embedding in paraffin. Then 4-μm-thick sections were processed for routine staining with hematoxylin-eosin, or with hematoxylin and periodic acid-Schiff (PAS).

Materials. Chemicals were purchased from Sigma (St. Louis, MO).

Statistical Analysis. Statistical analysis was performed by using an unpaired t test. When variances were not homogeneous, a Welch's correction was employed. P values less than .05 were considered significant. Values are expressed as means ± SEM. For these analyses, GraphPad (San Diego, CA) software was used.

Results

Bile duct ligation in rats ended in severe cholestasis, as indicated by increases of plasma levels of total and direct bilirubin. This corroborates the adequacy of the study design. Total bilirubin concentration in BDL rats increased to 44 ± 3 mg/L from 5 ± 0.5 mg/L ($P < .05$) observed in the sham group, whereas direct bilirubin level increased from 2 ± 0.2 mg/L in sham animals to 34 ± 4 mg/L in BDL rats ($P < .05$). Light microscopy only showed significant renal morphological alterations in PAS-stained kidneys. In BDL rats, renal tubules showed cells with PAS+ cytoplasmic granules. The height of the

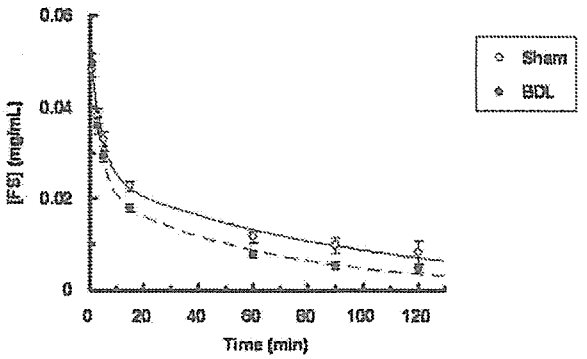

Fig. 1. Mean plasma concentration-time profile of FS in sham (n = 5) and BDL (n = 6) rats after a single 10 mg/kg, intravenous dose of FS. Results are expressed as means ± SEM.

epithelial cells and their apical folds were reduced. A few tubules resembled thyroid follicles because of the presence of PAS+ acidophilic material in their lumen (data not shown). These results are similar to those described by Wójcicki et al.[42]

Conversely, no significant difference was seen in urea serum levels (g/L) between sham-operated and BDL animals (0.41 ± 0.03 vs. 0.44 ± 0.04, respectively).

Mean plasma concentration-time profiles for FS in sham and BDL rats are shown in Fig. 1, and pharmacokinetic parameters are shown in Table 1. Lower plasma concentrations of FS in BDL group were displayed during the distribution and elimination phases. Therefore, BDL rats displayed a significant lower area under the curve and consequently a significant higher systemic clearance for FS. The elimination rate constant from the central compartment (K_{10}) was increased in BDL rats, indicating an alteration in the rate of elimination of FS. Distribution volumes were not significantly different between sham-operated and BDL animals. A statistically significant increase was observed in the quantity of FS excreted in urine during 120 minutes.

Table 1. Pharmacokinetic Parameters of FS in Sham (n = 5) and BDL (n = 6) Rats After a Single Dose (10 mg/kg Body Weight, Intravenously) of FS

	Sham	BDL
AUC (mg × min /mL)	2.64 ± 0.27	1.63 ± 0.14*
Cls (mL/min/100 g)	0.428 ± 0.067	0.636 ± 0.056*
K_{10} (min^{-1})	0.023 ± 0.003	0.038 ± 0.004*
VdT (mL/100 g)	38.16 ± 2.28	45.29 ± 4.86
VdC (mL/100 g)	18.54 ± 0.61	17.52 ± 1.50
VdP (mL/100 g)	19.61 ± 1.75	27.77 ± 3.67
Vdss (mL/100 g)	36.32 ± 2.06	41.46 ± 4.27
Amount of FS in urine (mg)	1.34 ± 0.19	1.90 ± 0.07*

NOTE. Results are expressed as means ± SEM.

Abbreviations: AUC, area under curve; Cls, systemic clearance; K_{10}, elimination constant from the central compartment, VdT, total volume of distribution; VdC, volume of the central compartment; VdP, volume of the peripheral compartment; Vdss, steady-state volume of distribution.

*$P < .05$.

Table 2. Glomerular Filtration Rate, Renal Clearance of FS, Excreted, Filtered, and Secreted Load of FS in Sham (n = 7) and BDL (n = 7) Rats

	Sham	BDL
Glomerular filtation rate (mL/min/100 g)	0.38 ± 0.07	0.43 ± 0.07
Renal clearance of FS (mL/min/100 g)	0.537 ± 0.049	0.739 ± 0.014*
Excreted load of FS (μg/min/100 g)	10.14 ± 0.94	13.93 ± 0.28*
Filtered load of FS (μg/min/100 g)	0.219 ± 0.034	0.242 ± 0.034
Secreted load of FS (μg/min/100 g)	9.93 ± 0.91	13.67 ± 0.30*

NOTE. Results are expressed as means ± SEM.

*$P < .05$.

FS binding to plasma proteins was approximately 97%, and there was no difference between both experimental groups (96.5 ± 0.55, n = 4 vs. 97.39 ± 0.30, n = 4, for sham and BDL rats, respectively).

Sham and BDL rats showed the expected diuretic and natriuretic response to FS. In sham rats, the UF (μL/min/100 g) increased from 4.8 ± 0.5 to 51.8 ± 5.8, $P < .05$, and the UENa (μEq/min/100 g) from 1.8 ± 0.2 to 8.5 ± 0.7, $P < .05$, in the absence and in the presence of FS, respectively. In BDL rats rats the UF (μL/min/100 g) increased from 9.0 ± 1.0 to 57.2 ± 2.9, $P < .05$, and the UENa (μEq/min/100 g) from 1.5 ± 0.3 to 9.1 ± 0.7, $P < .05$, in the absence and in the presence of FS, respectively. No statistical difference was seen between sham and BDL rats in UF and UENa after the administration of FS.

An increase in the renal clearance and in the excreted load of FS in BDL rats is shown in Table 2. The secreted load of FS was higher in BDL rats compared with sham rats. No significant difference was seen in filtered load of FS between sham-operated and BDL animals. The excreted load of FS was higher in BDL rats in consequence of the increase in the secreted load of this organic anion.

Na,K-ATPase activity (μmol Pi/h/mg protein) presented similar values both in kidney cortex homogenates (12.9 ± 1.6, n = 4 vs. 12.5 ± 1.9, n = 4) and in BLM (107 ± 3, n = 4 vs. 104 ± 2, n = 4) from BDL rats as compared with sham rats, respectively.

PAH uptake rate (nmol/15 sec/mg protein) was increased from 5.69 ± 0.28, n = 4 to 8.76 ± 0.78, n = 4, $P < .05$, in BLM vesicles from sham and BDL rats, respectively.

Kidney cortex homogenates and basolateral membranes from Sham and BDL animals were subjected to immunoblot analysis for OAT1 protein. Table 3 shows an increase of approximately 30% in OAT1 expression in homogenates from BDL rats as previously described.[14] As

Table 3. OAT1 and OAT3 Abundance in Cortex Homogenates From Kidneys of Sham and BDL Rats

	Sham	BDL
OAT1 (%)	100 ± 6	132 ± 7*
OAT3 (%)	100 ± 3	186 ± 19*

NOTE. Cortex homogenates (50 μg proteins) from kidneys of sham and BDL rats were separated by sodium dodecyl sulfate-polyacrylamide gel electrophoresis (8.5%) and blotted onto nitrocellulose membranes. OAT1 was identified using commercial polyclonal antibodies and OAT3 was identified using non-commercial polyclonal antibodies as described in Materials and Methods. Sham levels were set at 100%. Results are expressed as mean ± SEM from experiments carried out in triplicate on four different cortex homogenates preparations for each experimental group.

*$P < .05$.

shown in Fig. 2, a higher abundance of OAT1 of approximately 40% was observed in basolateral membranes from BDL rats as compared with sham rats. The OAT1 protein signal disappeared when the antibody was preabsorbed to the synthetic antigen peptide (data not shown).

Immunocytochemistry using HRP-conjugated secondary antibodies for light microscopy confirmed the increased OAT1 expression in basolateral plasma membranes from BDL rats (Fig. 3A-B). To further characterize the distribution of OAT1 labeling in proximal tubule cells, immunofluorescence was used (Fig. 3C-D). Confocal immunofluorescence studies also showed an increased OAT1 labeling in basolateral plasma membranes.

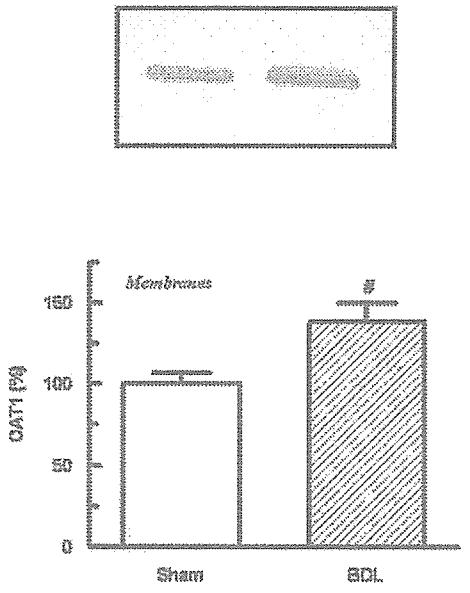

Fig. 2. (A) Renal basolateral membranes (40 μg proteins) from kidneys of sham and BDL rats were separated by sodium dodecyl sulfate-polyacrylamide gel electrophoresis (8.5%) and blotted onto nitrocellulose membranes. Membranes were stained with Ponceau Red to confirm equal protein loading and transfer between lanes. OAT1 was identified using commercial polyclonal antibodies as described in Materials and Methods. (B) Densitometric quantification of OAT1. For densitometry of immunoblots, samples from kidneys of BDL rats were run on each gel with corresponding sham kidney samples. Abundance was calculated as percentage of the mean sham control value for that gel. Sham levels were set at 100%. Each column represents mean ± SEM from experiments carried out in triplicate on four different cortex basolateral membranes preparations for each experimental group. #$P < .05$.

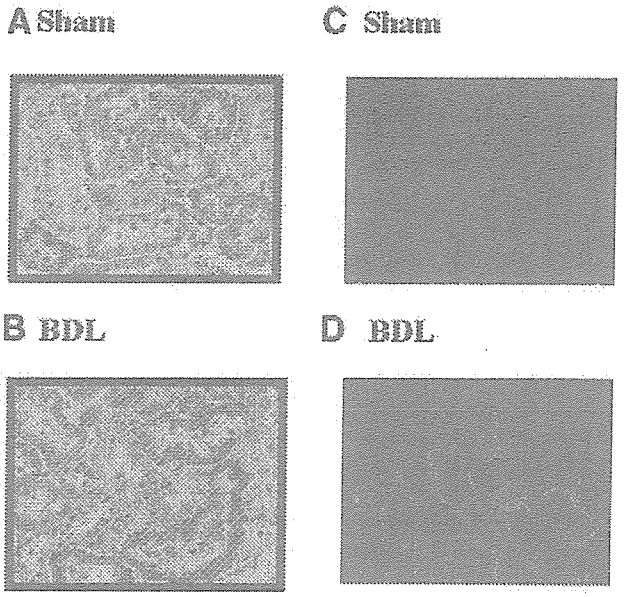

Fig. 3. Immunocytochemistry for OAT1 in the renal cortex of sham (A,C) and BDL rats (B,D). Serial sections from each rat kidney were stained using a non-commercial anti-rOAT1 antibody (crude immune serum). (A-B) Immunoperoxidase OAT1 labeling was seen at the basolateral domains of proximal tubule cells. In BDL rats, OAT1 labeling in BLM is greatly increased. (C-D) Immunofluorescence localization of OAT1. In BDL rats, increased labeling in BLM is seen. These figures are representatives of typical samples from four rats. Original magnification ×400.

Western blots of kidney cortex homogenates and BLM from sham and BDL rats showed signals for OAT3. Table 3 shows that OAT3 abundance was significantly increased in kidney cortex homogenates from BDL rats as compared with sham rats. In Fig. 4, it is possible to observe that there was no statistically difference in OAT3 abundance in BLM from both experimental groups. These signals were not observed when the antibody was preabsorbed with the OAT3 peptide (data not shown).

Immunocytochemistry studies showed staining for OAT3 in many parts of the nephron such as the proximal tubule (S1, S2, and S3) and the distal and collecting duct as was previously described.[2,35] Sham rats showed OAT3 labeling in basolateral membrane domain and inside the cytoplasm of renal tubular cells (Fig. 5A). Increased labeling was seen in the cytoplasm of tubules from kidneys of BDL rats (Fig. 5B). Immunofluorescence microscopy showed the basolateral membrane localization of OAT3, and the intracellular localization was better appreciated (Fig. 5C). An important increase of OAT3 inside the

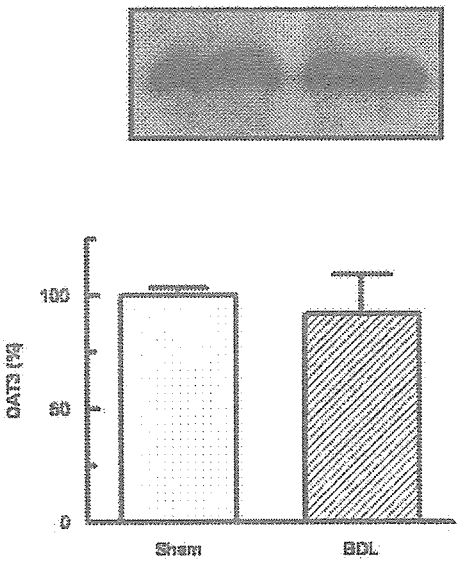

Fig. 4. (A) Renal basolateral membranes (40 μg proteins) from kidneys of sham and BDL rats were separated by sodium dodecyl sulfate polyacrylamide gel electrophoresis (8.5%) and blotted onto nitrocellulose membranes. Membranes were stained with Ponceau Red to confirm equal protein loading and transfer between lanes. OAT3 was identified using non-commercial polyclonal antibodies as described in Materials and Methods. (B) Densitometric quantification of OAT3. For densitometry of immunoblots, samples from kidneys of BDL rats were run on each gel with corresponding sham kidney samples. Abundance was calculated as percentage of the mean sham control value for that gel. Sham levels were set at 100%. Each column represents mean ± SEM from experiments carried out in triplicate on four different cortex basolateral membranes preparations for each experimental group. #$P < .05$.

cytoplasm was observed in cortex from kidneys of BDL rats (Fig. 5D). This pattern parallels the data from immunoblotting study.

Discussion

Numerous compounds, such as drugs, environmental substances, plant and animal toxins, and metabolites of both foreign and endogenous origins, are classified as organic anions. Because many of these substances are toxic to the body, their elimination is essential for homeostasis. The kidneys and liver are the major routes for organic anion elimination. In the kidneys, the transepithelial transport of organic anions occurs predominantly in proximal tubular cells.[6-8] OAT1 and OAT3 proteins are localized at the basolateral membrane of proximal tubular cells, and their substrate selectivity is markedly broad.[8-10,39,41] OAT1- and OAT3-mediated uptake of organic anions is driven by an outwardly directed concentration gradient of dicarboxylates such as a-ketoglutarate,[8] which depends on the correct function of the Na,K-ATPase bomb as both exchangers exhibit tertiary active transporter mechanism. The function of OAT1 and OAT3 in renal cells under physiological and pathological conditions has not been, as yet, fully elucidated. In this connection, we have described altered expression of OAT1 in kidneys from rats with bilateral ureteral obstruction,[35,37] arterial calcinosis,[27] and with chronic renal failure.[38] The regulation of renal organic anion transporters during cholestasis is poorly understood. However, defining the modifications of these transporters is important, both to understand the cholestatic process and to identify potential therapeutic targets.

An impaired liver function may induce some abnormalities in the kidney. Renal function in the course of obstructive jaundice has been the subject of great interest.[43]

All kinetic studies concerning elimination of drugs under mechanical cholestasis have been scarce and referred to the drugs mostly being metabolized in the liver or excreted into the bile.[42,44]

In the current study, we examined systemic and renal clearance of FS and the expression of both OAT1 and OAT3 in homogenates and basolateral membranes from rat renal cortex at 21 hours after ligation.

FS is a well-known loop diuretic secreted through the organic anion transport system. The capacity of the organic anion transport system to secrete a diuretic deter-

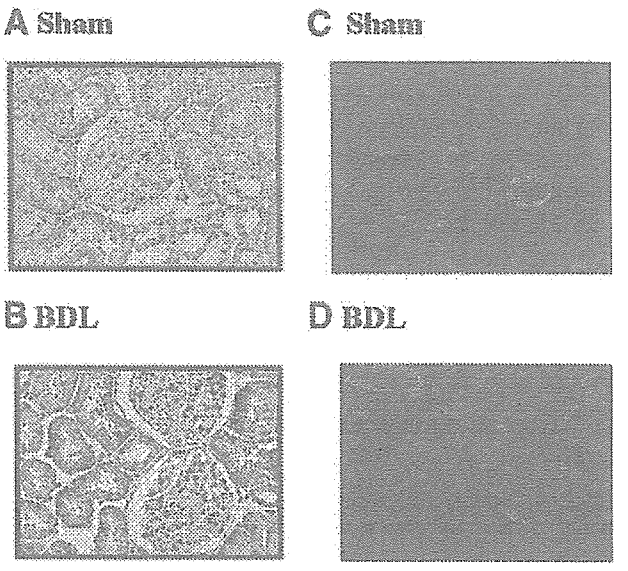

Fig. 5. Immunocytochemistry for OAT3 in the renal cortex of sham (A,C) and BDL rats (B,D). Serial sections from each rat kidney were stained using a non-commercial anti-rOAT3 antibody. (A-B) Immunoperoxidase OAT3 labeling was seen at the basolateral domains of tubule cells and inside the cells. In BDL rats, increased OAT3 labeling throughout the cytoplasm can be seen. (C-D) Immunofluorescence localization of OAT3. In BDL rats, increased OAT3 labeling can be seen throughout the cytoplasm of tubular cells. These figures are representatives of typical samples from four rats. Original magnification ×400.

mines its intraluminal concentration, which is critical for a diuretic activity.[17,19]

Our results have shown that rats at 21 hours after bile duct ligation exhibit a decrease in the area under the FS plasma concentration–time curve and an increase in total body clearance. A statistically different increase was observed in K_{10} in bile duct–ligated rats as compared with sham rats. K_{10} is influenced by variables that participate in the elimination of the drug from the central compartment, such as metabolization, renal, and biliary excretion.[45] The increase of K_{10} observed in BDL animals could indicate a higher renal elimination of this organic anion. This has been corroborated by the fact that rats subjected to BDL showed an increased FS renal clearance. The increase in renal FS clearance is accounted for by the increase in the secreted load of the drug, because the filtered load of FS was not modified in the BDL group. More studies are required for a better understanding of the correct dosage of drugs in patients with particular pathological states, such as extrahepatic cholestasis, as this work gives evidence of altered elimination of FS, a very useful loop diuretic in clinical medicine.

In our experimental BDL model, no difference was shown in Na,K-ATPase activity. The protein expression of OAT1 was significantly increased both in cortical homogenates and in basolateral membranes from kidneys after 21 hours of BDL, which might suggest an increase in the synthesis or a decrease in the degradation of these membrane transporters. This OAT1 upregulation might lead to a higher elimination of its transported compounds. In this connection, PAH uptake rate was increased in BLM from BDL rat vesicles. Like FS, PAH is transported by OAT1.[6-8] In this study, OAT1 up-regulation was associated with a concomitant increase of systemic and renal FS clearance.

At variance with OAT1, OAT3 expression only increased in homogenates and not in BLM from BDL kidneys, suggesting an increase in synthesis or a decrease in degradation without an increase of the recruitment of preformed transporters into membranes. The intracellular granular staining observed for OAT3 in both sham and BDL rats (physiological and pathological conditions) indicates the localization of the protein in a vesicle population that may be involved in the recycling of this transporter by means of endocytosis and exocytosis, similar to that described by Villar et al[35] and by Ljubojevic et al.[46]

Loop diuretics reach the NKCC2 transporters that are inserted into the luminal membrane by being actively secreted from the blood into the urine at the proximal tubule by means of the organic anion transporters. One factor that conditions the delivery of diuretics to their site of action is the renal blood flow. We have previously shown that rats after 21 hours of BDL show a decrease in renal blood flow.[14] Nevertheless, with the reduction of the fraction of an administered dose of FS that is presented to the kidneys from BDL rats, we observed an increased renal elimination of FS, which indicates the importance of the increased OAT1 abundance in BLM from treated rats.

Our results showed an upregulation of OAT1 and OAT3 in homogenates. In this connection, extrahepatic cholestasis is associated with production of various cytokines and growth factors that may affect gene transcription.[47] Similarly, with OAT1 and OAT3, MRP2 upregulation in BDL rats was described by Tanaka et al.[13] These authors found that bilirubin ditaurate, sulfate-conjugated bile acids, and some components of the human bile upregulate the expression of MRP2 in human renal tubular cells. As highly accumulated anionic drugs observed during cholestasis may cause a general body deterioration, the molecular mechanism(s) involved in the upregulation of MRP2, OAT1, and OAT3 expression should be elucidated to improve drug elimination under this pathological condition.

Extrahepatic cholestasis induces a complex series of hormonal changes in kidneys,[1-4] which might influence the regulation of OAT1 and OAT3. Likely several local and systemic factors are produced at the same time, and the role of such factors in the regulation of channels and transporters in the presence of BDL is unknown.

Further research also should be directed toward delineation of the molecular basis for transcriptional, translational, and post-translational regulation of OAT1 and OAT3 both in physiological and pathological conditions, because of their impact on the efficiency of the kidneys in excreting endogenous and exogenous anionic compounds.

Optimal therapeutic use of loop diuretics requires an understanding of their basic pharmacology (pharmacokinetics and pharmacodynamics, both in physiological and pathological states) and how that translates to clinical pharmacology. Whether a patient should receive diuretics, and, if so, what therapeutic regimen should be used, depends on the clinical situation. Loop diuretics can be used to treat a wide variety of therapeutic cases (edematous conditions, congestive heart failure, cirrhosis of the liver, and nephrotic syndrome). If these patients also suffer extrahepatic cholestasis, care must be taken when FS is administered.

We have shown that the secreted load of FS is increased in rats with extrahepatic cholestasis as compared with

sham rats, after the administration of the same dose of FS. Nevertheless, an increase in the diuretic and natriuretic effects of FS in BDL rats was not seen. Intraluminal FS concentrations obtained both in BDL and Sham rats may have both been maximal inhibitory concentrations for the NKCC2 cotransporter, or function or abundance of this carrier may have been modified in BDL rats. To elucidate this issue, new experiments are currently being performed in our laboratory.

Acknowledgment: The authors thank Alejandra Martínez (Facultad de Ciencias Bioquímicas y Farmacéuticas, UNR) for her technical assistance. The authors also thank Wiener Lab Argentina for analytical kits.

References

1. Koopen NR, Müller M, Vonk RJ, Zimniak P, Kuipers F. Molecular mechanisms of cholestasis: causes and consequences of impaired bile formation. Biochim Biophys Acta 1998;1408:1-17.
2. Reichen J, Simon FR. Cholestasis. In: Arias MI, Jakoby WB, Popper H, Schachter D, Shafritz DA, eds. The Liver: Biology and Pathobiology. 2nd ed. New York: Raven Press, 1988:1105-1124.
3. Kramer HJ. Impaired renal function in obstructive jaundice: roles of the thromboxane and endothelin systems. Nephron 1997;77:1-12.
4. Wait RB, Kahng KU. Renal failure complicating obstructive jaundice. Am J Surg 1989;157:256-263.
5. Fleck Ch, Bräunlich H. Renal handling of drugs and amino acids after impairment of kidney or liver function-Influences of maturity and protective treatment. Pharmacol Ther 1995;67:53-57.
6. Wright SH, Dantzler WH. Molecular and cellular physiology of renal organic cation and anion transport. Physiol Rev 2004;84:987-1049.
7. Burckhardt G, Wolff NA. Structure of renal organic anion and cation transporters. Am J Physiol 2000;278:F853-F866.
8. Sweet DH, Bush KT, Nigam SK. The organic anion transporter family: from physiology to ontogeny and the clinic. Am J Physiol 2001;281:F197-F205.
9. Cha SH, Sekine T, Fukushima J-I, Kanai Y, Kobayashi Y, Goya T, et al. Identification and characterization of human organic anion transporter 3 expressing predominantly in the kidney. Mol Pharmacol 2001;59:1277-1286.
10. Sekine T, Watanabe N, Hosoyamada M, Kanai Y, Endou H. Expression cloning and characterization of a novel multispecific organic anion transporter. J Biol Chem 1997;272:18526-18529.
11. Smeets PH, van Aubel RA, Wouterse AC, van den Heuvel JJ, Russel FG. Contribution of multidrug resistance protein 2 (MRP2/ABCC2) to the renal excretion of p-aminohippurate (PAH) and identification of MRP4 (ABCC4) as a novel PAH transporter. J Am Soc Nephrol 2004;15:2828-2835.
12. Van Aubel R, Peters JG, Masereeuw R, Van Os CH, Russel FGM. Multidrug resistance protein Mrp2 mediates ATP-dependent transport of classical renal organic anion p-aminohippurate. Am J Physiol 2000;279:F713-F717.
13. Tanaka Y, Kobayashi Y, Gabazza EC, Higuchi K, Kamisako T, Kuroda M, et al. Increased renal expression of bilirubin glucuronide transporters in a rat model of obstructive jaundice. Am J Physiol 2002;282:G656-G662.
14. Brandoni A, Quaglia NB, Torres AM. Compensation increase in organic anion excretion in rats with acute biliary obstruction: role of the renal organic anion transporter 1. Pharmacology 2003;68:57-63.
15. Jackson E. Diureticos. In: Hardman JG, Limbird LE, Molinoff PB, Ruddon RW, Goodman Gilman A, eds. Las Bases Farmacológicas de la Terapéutica. 9th ed. Mexico: McGraw-Hill Interamericana, 1996:735-766.
16. Okusa MD, Ellison DH. Physiology and pathophysiology of diuretics. In: Seldin DW, Giebisch G, eds. The Kidney Physiology and Pathophysiology. Philadelphia: Lippincott Williams & Wilkins, 2000:2877-2922.
17. Hasannejad H, Takeda M, Taki K, Shin HJ, Babu E, Jurabha P, et al. Interactions of human organic anion transporters with diuretics. J Pharmacol Exp Ther 2004;308:1021-1029.
18. Kusuhara H, Sekine T, Utsunomiya-Tate N, Tsuda M, Kojima R, Cha SH, et al. Molecular cloning and characterization of a new multispecific organic anion transporter from rat brain. J Biol Chem 1999;274:13675-13680.
19. Uwai Y, Saito H, Hashimoto Y, Inui KI. Interaction and transport of thiazide diuretics, loop diuretics, and acetazolamide via rat renal organic anion transporter r OAT1. J Pharmacol Exp Ther 2000;295:261-265.
20. Cerrutti JA, Quaglia NB, Brandoni A, Torres AM. Effects of gender on the pharmacokinetics of drug secreted by the renal organic anions transport systems in the rat. Pharm Res 2002;45:107-112.
21. Cerrutti JA, Quaglia NB, Torres AM. Characterization of the mechanisms involved in the gender differences in p-aminohippurate renal elimination in rats. Can J Physiol Pharmacol 2001;79:805-813.
22. Quaglia NB, Hofer CG, Torres AM. Pharmacokinetics of organic anions in rats with arterial calcinosis. Clin Exp Pharmacol Physiol 2002; 29:48-52.
23. Shumaker R. PKCALC: a basic interactive computer program for statistical and pharmacokinetic analysis of data. Drug Metab Rev 1986;17:331-348.
24. Motulsky H. Using nonlinear regression to fit curves. In: Motulsky H, ed. Intuitive Biostatistics. New York: Oxford University Press, 1995: 227-283.
25. Bratton AC, Marshall EK Jr. Determination of p-aminohippurate. J Biol Chem 1939;128:537-542.
26. Brandoni A, Villar SR, Torres AM. Gender-related differences in the pharmacodynamics of furosemide in rats. Pharmacology 2004;70:107-112.
27. Quaglia NB, Brandoni A, Ferri A, Torres AM. Early manifestation of nephropathy in rats with arterial calcinosis. Renal Fail 2003;25:355-366.
28. Quaglia NB, Brandoni A, Villar SR, Torres AM. Haemodynamic and tubular renal dysfunction in rats with sustained arterial calcinosis. Clin Exp Pharmacol Physiol 2004;31:231-236.
29. Roe HH. A photometric method for determination of inulin in plasma and urine. J Biol Chem 1949;178:839-844.
30. Jensen RE, Berndt WO. Epinephrine and norephinephrine enhance p-aminohippurate transport into basolateral membrane vesicles. J Pharmacol Exp Ther 1988;244:543-549.
31. Cerrutti JA, Brandoni A, Quaglia NB, Torres AM. Sex differences in p-aminohippuric acid transport in rat kidney: role of membrane fluidity and expression of OAT1. Mol Cell Biochem 2002;233:175-179.
32. Schoner W, Von Ilberg C, Kramer R, Seubert W. On the mechanism of Na+ and K+ stimulation hydrolysis of adenosine triphosphate. Eur J Biochem 1967;1:334-343.
33. Widnell CB. Purification of rat liver 5'nucleotidase as a complex with sphingomyelin. Methods Enzymol 1974;32:368-374.
34. Torres AM, MacLaughlin M, Quaglia NB, Stremmel W. Role of BSP/bilirubin binding protein on p-aminohippurate transport in rat kidney. Mol Cell Biochem 2003;248:149-156.
35. Villar SR, Brandoni A, Anzai N, Endou H, Torres AM. Altered expression of rat renal cortical OAT1 and OAT3 in response to bilateral ureteral obstruction. Kidney Int 2005,68:2704-2713.
36. Sedmak JJ, Grossberg SE. A rapid, sensitive and versatile assay for protein using Coomassie Brilliant Blue G250. Anal Biochem 1977;79: 544-552.
37. Villar SR, Brandoni A, Quaglia NB, Torres AM. Renal elimination of organic anions in rats with bilateral ureteral obstruction. Biochim Biophys Acta 2004;1688:204-209.
38. Torres AM, MacLaughlin M, Muller A, Brandoni A, Anzai N, Endou H. Altered renal elimination of organic anions in rats with chronic renal failure. Biochim Biophys Acta 2005;1740:29-37.

39. Tojo A, Sekine T, Nakajima N, Hosoyamada M, Kanai Y, Kimura K, et al. Immunohistochemical localization of multispecific renal organic anion transporter 1 in rat kidney. J Am Soc Nephrol 1999;10: 464-471.
40. Shah V, Cao S, Hendrickson H, Yao J, Katusic ZS. Regulation of hepatic eNOS by caveolin and calmodulin after bile duct ligation in rats. Am J Physiol 2001;280:G1209-G1216.
41. Kojima R, Sekine T, Kawachi M, Cha SH, Suzuki Y, Endou H. Immunolocalization of multispecific organic anion transporters, OAT1, OAT2, and OAT3, in rat kidney. J Am Soc Nephrol 2002;13: 848-857.
42. Wójcicki M, Drozdzik M, Sulikowski T, Wójcicki J, Gawronska-Szklarz B, Zielinski S, et al. Pharmacokinetics of intravenously administered digoxin and histopathological picture in rabbits with experimental bile duct obstruction. Eur J Pharm Sci 2000;11:215-222.
43. Sitprija V, Kasbemsant U, Sriratanban A, Arthachinta S, Poshyachinda V. Renal function in obstructive jaundice in man:cholangiocarcinoma model. Kidney Int 1990;38:948-9555.
44. Miyazawa Y, Sato T, Kobayashi K, Akahori F, Suzuki T, Miyashita H. Influence of induced cholestasis on pharmacokinetics of digoxin and digitoxin in dogs. Am J Vet Res 1990;51:605-610.
45. Wilkinson GR. Clearance approaches in pharmacology. Pharmacol Rev 1987;39:1-47.
46. Ljubojevic M, Herak-Kramberger CM, Hagos Y, Bahn A, Endou H, Burckhardt G, et al. Rat renal cortical OAT1 and OAT3 exhibit gender differences determined by both androgen stimulation and estrogen inhibition. Am J Physiol 2004;287:F124-F138.
47. Plebani M, Panozzo MP, Basso D, De Paoli M, Biasin R, Infantolino D. Cytokines and the progression of liver damage in experimental bile duct ligation. Clin Exp Pharmacol Physiol 1999;26:358-363.